ABSTRACT

COMPUTER AIDED FINITE ELEMENT STRESS ANALYSIS OF A THREE DIMENSION MANDIBULAR BONE MODEL Using I-DEAS Software

by
Yixiong Xu

A three dimensional model of half of the mandibular bone, with 487 tetrahedra elements and 1,047 nodes, is established and analyzed by means of I-DEAS software. The masseter muscle is assumed to be 15° deviation from y-axis, and the Umetani boundary conditions are allowed to be varied. A 337 lb force was applied along the midline of the mandible to simulate a trauma force caused by the auto accident. The maximum principal stress is 18,400 psi and the minimum principal stress is -1,340 psi. Depending on the experimental results of dispalcement and maximum principal stress, the conclusions are drawn: 1) mandibular body and angle may have the highest probability of fracture, 2) the mandible is under compressive stress and of the compressive displacement. There are maximum stress concentration occured in the condyle process area and the coronoid process area. The results are approximately agreed with the clinic investigation of 1,521 series of mandibular bone fractures.

COMPUTER AIDED FINITE ELEMENT STRESS ANALYSIS OF A THREE DIMENSION MANDIBULAR BONE MODEL Using I-DEAS Software

by
Yixiong Xu

A Thesis
Submitted to the Faculty of the New Jersey Institute of Technology
in Partial Fulfillment of the Requirements for the Degree of
Master of Science
in Biomedical Engineering
January, 1993

Approval Page

Computer Aided Finite Element Stress Analysis of A Three Dimension Mandibular Bone Model Using I-DEAS Software

by
Yixiong Xu

8/31/92

Dr. David Kristol, Thesis Adviser
Director of Biomedical Engineering Program
Professor of Chemical Engineering, Chemistry, and Environmental Science, NJIT

8/31/92

Dr. Frank Shih, Committee Member
Assistant Professor of Computer and Information Science, NJIT

9/1/92

Dr. Timothy Chang, Committee Member
Assistant Professor of Electrical Engineering, NJIT

BIOGRAPHICAL SKETCH

Author : Yixiong Xu

Degree : Master of Science in Biomedical Engineering

Date: January, 1993

Date of Birth:

Place of Birth:

Undergraduate and Graduate Education:

- Master of Science in Biomedical Engineering, New Jersey Institute of Technology, Newark, NJ, 1993

- Bachelor of Science in Physics, Xiamen University, Xiamen, Fujian P. R. China

Major: Biomedical Engineering

This thesis is dedicated to my wife

Qingyou Yan

and

my parents

Acknowledgement

This author wishes to express his sincere gratitude to his adviser, Professor David Kristol, for his guidance, friendship and moral support throughout this research. Special thanks to Dr. Frank Shih and Dr. Timothy Chang for serving as members of the committee.

The author appreciates the timely help and suggestions from Dr. Martin Linden, Dr. Clarence Mayott, Mr. Wei. C. Chang and Mr. Don Rosander.

TABLE OF CONTENTS

Page

Page

Page

List Of Tables

LIST OF FIGURE

Figure **Page**

Figure	Page

Chapter 1
Introduction

1.1 Review of Finite Element Application in Dental Sciences

The finite element method is a computerized numerical iteration technique used to determine the stresses and displacements throughout a predesigned model. The method was first introduced in the late sixties in the aerospace industry, and was applied in dentistry in the early seventies by Farah, Craig and Sikarshi [1] to optimize the design of dental restorations. Although the finite element method was even used to study the stress between the dentine and enamel[2], studies for mandible are relatively fewer due to its complicated geometry shape and mastication system muscles.

Knoll, *et al.* [3] used a three dimensional finite element model of a mandible to calculate strain from the region of the first biscuspid to the first molar. The main improvement over an earlier study by Gupta, Knoell and Grenoble [4] was an improved model of the bone supporting the dentition. The mechanical properties of the cancellous bone were developed by scaling the properties of cortical bone on the basic of porosity found with mandibular sections.

1.2 Review of Mastication System Muscles Pattern

The mastication system of human beings consists of four pairs of muscles. They are the masseter muscle, temporalis muscle, medial and lateral pterygoid muscles. The performance of mastication muscles has been studied by using mathematical models and analytical methods. In the early sixties, electromyography (EMG) was widely used in the study of the relative activity of mastication muscles. Such studies can only crudely measure activity in terms of how actively a muscle is working rather than the amount of force it is producing.

Weijs [5] *et al.* made a landmark progress in 1985, they discovered that intrinsic muscle strength is between $0.3 \times 10^6 Nm^{-2}$ and $0.4 \times 10^6 Nm^{-2}$. This property has not only been found in voluntary muscle contraction in human beings, but also in animals during stimulated contraction experiments. Using computer tomography (CT) scan technique, Weijs [6] also measured the physiological cross section (PCS) of muscle. In 1992, Koolstra *et al.* [7], using the magnetic resonance imaging (MRI) method, claimed that they obtained more accurate data of PCS than Weijs did, due to the better contrast of MRI technique.

1.3 Review of Mechanical Analysis of Mandible

Jadranka [8] established an approximate model of the mandible, using the photoelastic method to measure the deformation and strain when an extensor force was applied in the alveolar area of the lower jaw bone. The article focused on discussing the force created by orthodontics. Photoelasticity requires the use of a transparent model of the structure to study, so it does not accurately reproduce the mechanical properties.

Later, Ferre, *et al.* [9] established a physicomathematical mandible model, which was assumed isolated and under static constraints. Using optical interferometry to observe the deformation results, when constraints were applied to the fresh mandible taken from an unembalmed cadaver, they concluded that the mandible under compressive force presents the complex phenomenon of a spiral force that changes direction at each "fusible" area. However, the authors omitted the muscular environment with the mandible suspended in the space by its suspensory organ (such as mastication system muscles and tendons), also the computer program was altered to amplify the deformations occuring in the model. Therefore, the study results are qualitative instead of being quantitative.

In 1988, Umetani, *et al.* [10] developed a model concerning the movement of the mandible under the frontal compressive load. They concerned that the condyloid process was a hinge connection, the coronoid process was under the restraint force of temporalis muscle, the second molar area was fixed in y-axis direction, and the angle was under the muscle, the second molar area was fixed in y-axis direction, and the angle was under the restraint force of masseter muscle. They did not however give the value of forces which were used as boundary condition. Concerning the mandible as a linear beam, by using COSMOS 6 software to solve the problem, they concluded that the upper part of the mandible was under compression stress and the lower part was under tension stress. The deformation was exaggerated to demonstrate its distribution. Both the value of stress and deformation were not given.

Among the several studies of the elastic properties of mandibular bone, an important one is by Ashman and Van Buskirk [13]. Using an advanced ultrasound technique they measured the nine independent orthotropic elastic constants. They concluded that human mandibular bone is elastically homogeneous but aniostropic; it acts like a long bone bent into the shape of a horseshoe.

In 1985, Pantelis Nic [31] reviewed a series of 1,521 mandibular fractures. The major cause of the mandibular fractures in his study was motor vechicle accidents (52.5%). The anatomic distribution of fractures was given. The fractures of the mandibular body were the most common (41.5%). Fractures of the angle accounted for 23.7% and of the condyloid process for 23.1%.

1.4 Purpose of Current Research

Hart, R.T. *et al.* [14] developed a three dimensional finite element study of a partial edentulated human mandible to calculate the mechanical response to simulated isometric biting and mastication loads. Using the property of transverse isotropy [13] of the mandible, they obtained some successful results. Some problems still have not been solved, such as the detailed knowledge regarding the material property of cancellous bone and the uncertainty of how to realistically distribute the muscle loading and the difficulty of knowing how to model the boundary conditions at the condyles.

Although all the problems mentioned above still exist, the purpose of this thesis is to tribution and deformations under certain simulated boundary conditions. The structural load in the boundary condition is simulated as a force caused by automobile accident. Then the results are used to compare with the Pantelis's clinical statistical investigation of facial fracture distribution [31].

Chapter 2
Basic Computer Aided Design of the Finite Element Method

2.1 General Structure

In computer aided design (CAD) the determination of the performance (e.g. stress or deformation) of a device using the finite element method (FEM) during its design process is accomplished by analysis of the partial differential equations which describe the given system [17, 18]. This involves the following three steps (see Figure 2.1): (1) the description of the geometry, the physical characteristics and the mesh; (2) the application of the FEM; (3) the visualization and interpretation of the results of the simulation.

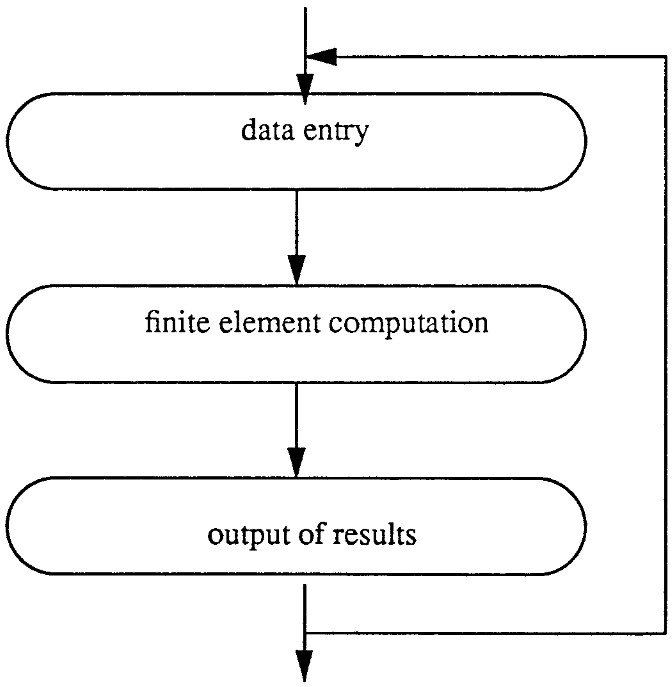

Figure 2.1 Flow Chart of the Operation of A Finite Element Program

These three steps are quite distinct and correspond to developing on the programming level, the three distinct modules are: (1) the module to enter the data; (2) the module to perform the analysis; (3) the module to analyze the results.

2.2 The Data Entry Module

The data entry module is used for entering the information necessary for analysis of the problem by FEM. This data relates to the discretization of the domain and the representation of its physical behaviour.

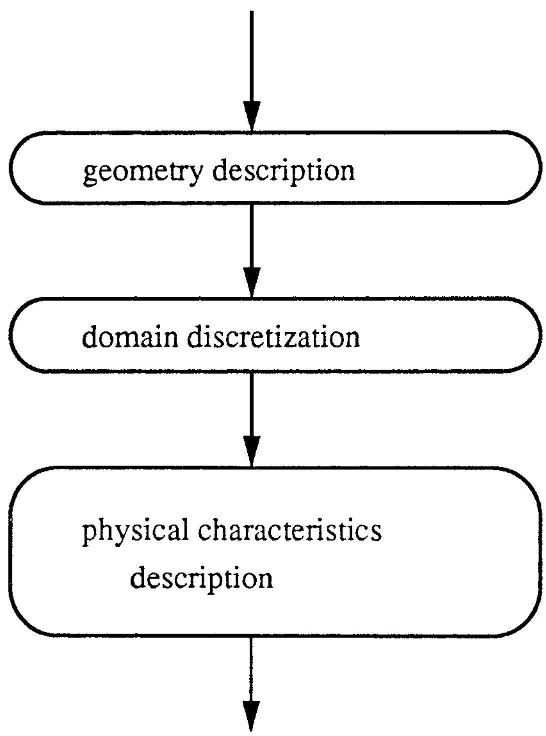

Figure 2.2 Data Entry Function

The data entry module must accomplish the following three functions: (1) description of the geometry of the object; (2) mesh generation; (3) definition of the regions and the boundaries. The mesh generation consists of finding a collection of nodes and a collection of finite elements which form an acceptable discretization of the domain.

Such a discretization must respect the boundaries of the domain and interfaces between two regions. The shape of the finite elements must not be too irregular (elongated) and should, as much as possible, resemble the reference elements (equilateral triangles or tetrahedra, squares or cubes, etc.). The nodes are defined by their coordinates while the elements are characterized by their type and a list of their nodes. Certain formulations involve boundary integrals, not only interior finite element (volume elements in three dimensions, surface elements in two) but also boundary finite elements in three dimensions (surface elements in three dimensions, line elements in two) on the corresponding boundaries must be constructed.

The operation of constructing elements in regions and on boundaries also presents the opportunity to describe the physical characteristics, such as: the material properties (e.g. Young modulus); sources (e.g. structural loads); and boundary conditions (for time dependent or time independent problems).

The description of geometry is sometimes implicitly linked to the meshing, however, the trend at present is to separate the two. The description of the geometry is done first and then the mesh is generated. The most extreme case of this separation is the use of two separate specialized programs (see Figure 2.2): a solid modeller for the geometrical input (for example, I-DEAS, Finite Element Modeling & Analysis, Geometry Modeling) and a mesh generator for the discretization displacement (for example, I-DEAS, Finite Element Modeling & Analysis, Mesh Creation).

2.3 The Solver

The solver computes the unknowns in a finite element problem, i.e. it solves the linear or non-linear system of equations coming from the variational or the projective formulation. Its input is the domain discretization, the physical characteristics and the boundary conditions. The output is the value of the unknown force or displacement at each of the nodes of the grid.

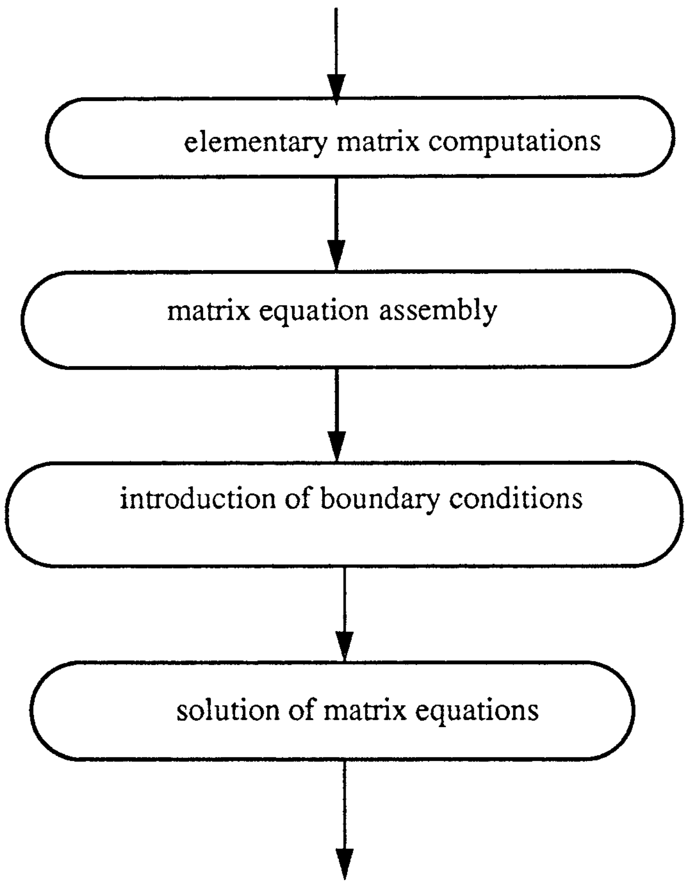

Figure 2.3 Solver: Operations for A Linear Static Problem

Two large classes of methods are used to solve these sets of equations: point or block methods of relaxation or global matrix methods. The latter, more popular today, requires several steps: (1) creation of sub-matrices and subvectors corresponding to each individual finite element; (2) assembly of these elementary matrices and vectors to build the system matrix and right hand vector; the bigger the system assembly matrix, the more powerful and expensive the software. (3) solution of the linear system of equations.

Unlike ANSYS installed in NJIT, which has the limitation of at most 500 matrix elements, I-DEAS does not have the limitation. However, the memory space and CPU time needed in the Sun workstation is still a problem when creating a mesh with a larger amount of elements.

The solution of linear algebraic systems can be performed in several ways; by direct methods (Gauss, Choleski), semi-direct methods (ICCG), or block iterative methods (Gauss-Seidel). When the system of equations is non-linear, these operations are repeated in an iterative scheme (Gauss-Seidel, Newton-Kantorovich, Newton-Raphson; Figure 2.4). When the problem is time dependent, these steps must be repeated for each time step (implicit or explicit finite difference methods. Crank-Nicholson, Predictor-Corrector) until the operating time of the program is equal to or larger than the time dependent range of the problem.

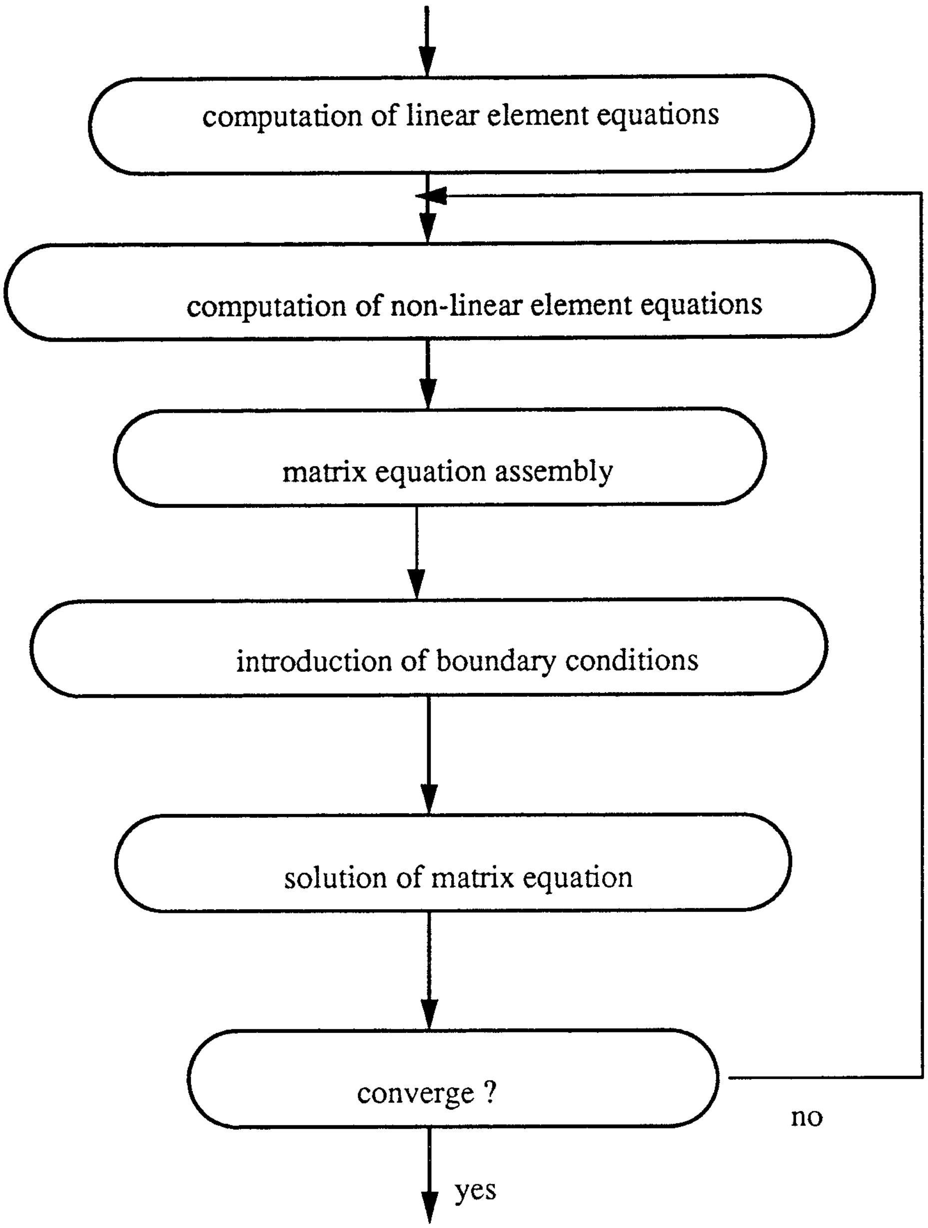

Figure 2.4 Solver: Operations for A Non-linear Static Problem

2.4 Postprocessors

The postprocessor solves the above problem by the computational modules (see Figure 2.5). However, the results are not always useful because of the following reasons: the state variables, computation at the finite element nodes, description of the state of the system in mathematical form. Sometimes the physical meaning is not clear; the large amount of data coming from the solver (several thousands of nodal values) are often too much to be understood without further processing.

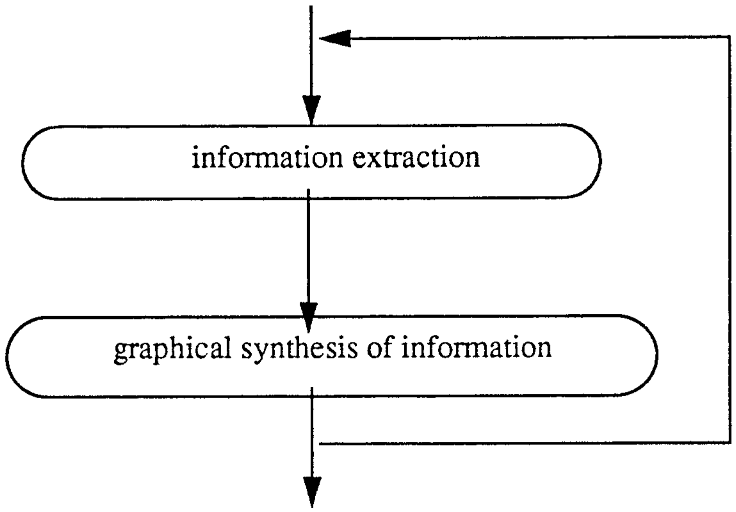

Figure 2.5 Postprocessor Functions

The postprocessor (see Figure 2.5) performs two tasks: (1) extraction of significant information, and (2) graphically presents the results. The information may be related to local quantities (displacement) or global quantities (structural stress, etc). The graphical output makes the data more understandable and easier to interpret (field plots, isostrain plots, stress vs time curves time curves, etc.)

2.5 Summary

Although advanced finite element analysis softwares (e.g. Flux3d, Euclid, Nastran, ANSYS, I-DEAS, etc.) may have different complicated architecture of the program (e.g. the communication between the several programs at the same module level), the basic and principal steps and principles are almost same, as the descriptions above.

As the FEM software package of CAD, both ANSYS and I-DEAS are usually used as standard software for post-processing. The description of the model by common language (e.g. Fortran) or special language (e.g. ANSYS or I-DEAS programming language) is accepted by the two softwares. However, ANSYS is based on the function of finite element analysis (it is of rapid calculation speed.) while I-DEAS is based on the function of finite element modeling (it is able to describe the complicated object.). In this study, I-DEAS was used to establish the finite element model and show the results of the analysis when ANSYS was used as an assistant finite element analysis to run the intermediate test program.

Chapter3
Anatomy of Mandibular Bone and Mastication System Muscles

In FEM there are three important factors which determine the stress and deformation pattern of the object studied. These are the material property, physical property and boundary condition of the object. In the field of biomechanics, these factors were usually obtained by making some simplifications after studying and discussing the anatomic and physiological details of the bio-object. The anatomy of the mandible and the mastication system muscles will be discussed in the following sections.

3.1 Description of Mandibular Bone

The mandible (see Figure 3.1 [20]) is the largest and strongest bone of the face [19,20,21]. It supports the inferior teeth and articulates in the mandibular fossae of the temporal bones. It consists of a horizontally curved body, resembling a horseshoe in shape, from each end of which a ramus ascends almost at a right angle. The body of the mandible is marked in the midline anteriorly by a faint groove or ridge that indicates the place of union of the two originally separated halves of the bone. This ends inferiorly in the elevation of the chin known as the mental protuberance, which is slightly depressed in the center and on each side is raised to form a mental tubercle. On the external surface, related to the incisor teeth, are alveolar ridges from which the mentalis and deep fascicles of the orbicularis oris muscles arise. More laterally, opposite the second premolar and midway between the superior and inferior margins, is the mental foramen, used for the mental nerve and vessels. Inferior to the foramen is the somewhat indefinite oblique line, extending from the mental tubercle to the anterior border of the ramus; the portion inferior to the line affords origin to the depressor labbi interioris and the depressor anguli oris muscles.

The internal surface presents in the midline some small projections, or genial tubercles, forming the mental spine. These tubercles are often arranged in two pairs, one superior to the other; the prominent superior one gives origin to the genioglossus muscle, and the inferior, represented in some bones by a median ridge or only a slight roughness, gives origin to the geniohyoid muscle. Near the inferior margin on either side is an oval depression, the digastric fossa, for the attachment of the anterior belly of the digastric muscle.

The ramus of the mandible is quadrilateral in shape. The lateral surface is flat, gives insertion into the masseter muscle, and at the inferior part is marked by several oblique ridges for the attachment of tendinous bundles in the substance of the masseter. Near the middle of medial surface is the mandibular foramen leading into the mandibular canal. The posterior border of the ramus is thick and rounded; in meeting the base it forms the angle of the jaw, which is approximately 122° in the adult. The angle is rough and usually everted. The anterior border passes into the oblique line of the external surface of the body and merges with a triangular surface posterior to the third molar tooth. Here a short ridge is often present, giving attachment to the buccinator muscle. The superior border presents two processes: anteriorly the coronoid process and posteriorly the condylar process. They are separated by a deep concavity, the mandibular notch.

The condylar process consists of the condyle and the narrowed portion by which it is supported, the neck. The mandibular condyl is ovoid in form, has its long axis transverse to the ramus but is oblique to the median axis of the skull; the lateral extremity is a little anterior to the level of the medial extremity. The neck is flattened anteroposteriorly and presents, anteriorly, the pterygoid fossa for the insertion of the lateral pterygoid muscle.

The coronoid process, flattened and triangular, projects superiorly from the anterior part of the ramus, usually to a somewhat higher level than that reached by the condylar process. Its lateral surface is smooth and gives insertion to the temporal and masseter muscles; the medial surface is marked by a ridge that descends from the tip and becomes continuous with the posterior part of the mylohyoid line.

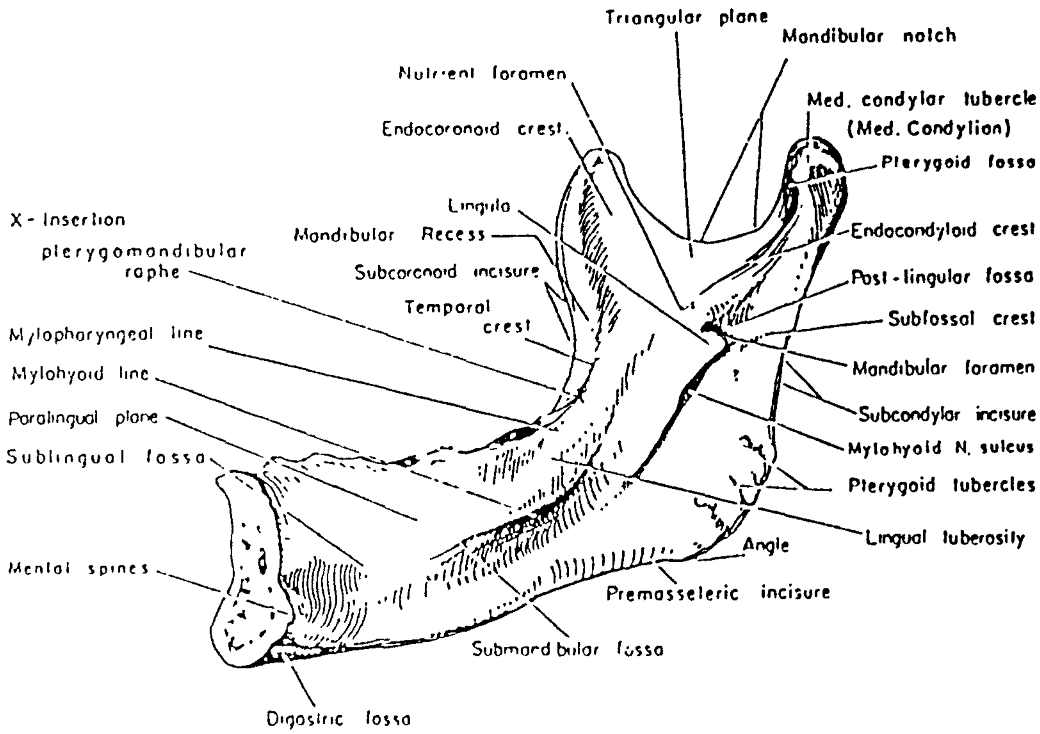

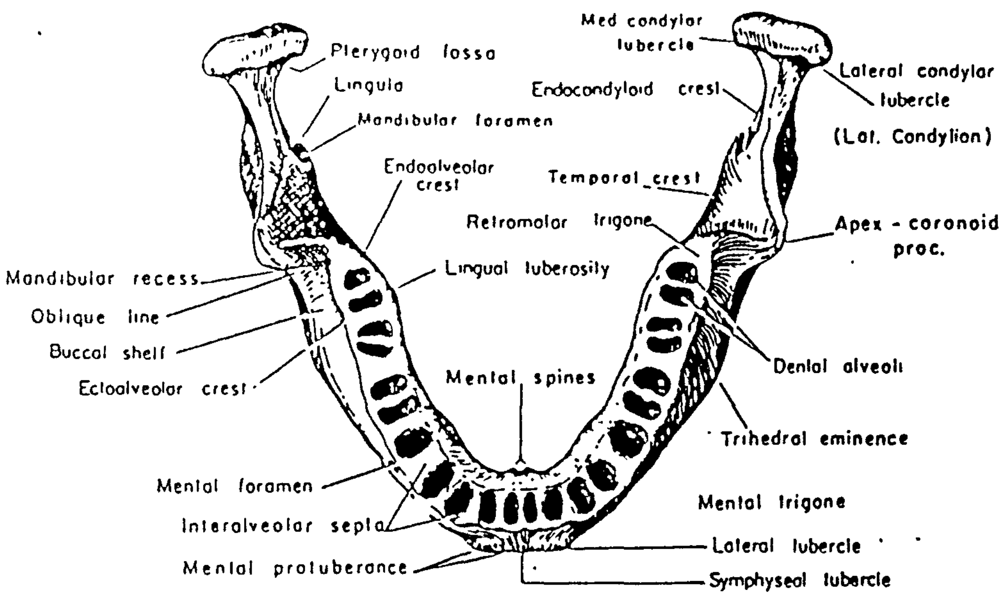

Figure 3.1 Mandibular Bone [20]

According to Huelke [20] , in the areas of condyle process and coronoid process, the cortical bone is thiner, see Figure 3.2. The transverse compressive yield strength of cortical bone is 133 Mpa, and that of cancellous bone is 14.0-5.3 Mpa [34]. Since the coxtical bone is almost of as 10-25 times strength as cancellous bone, the condyle process and coronoid process are the weak areas in the mandibular bone.

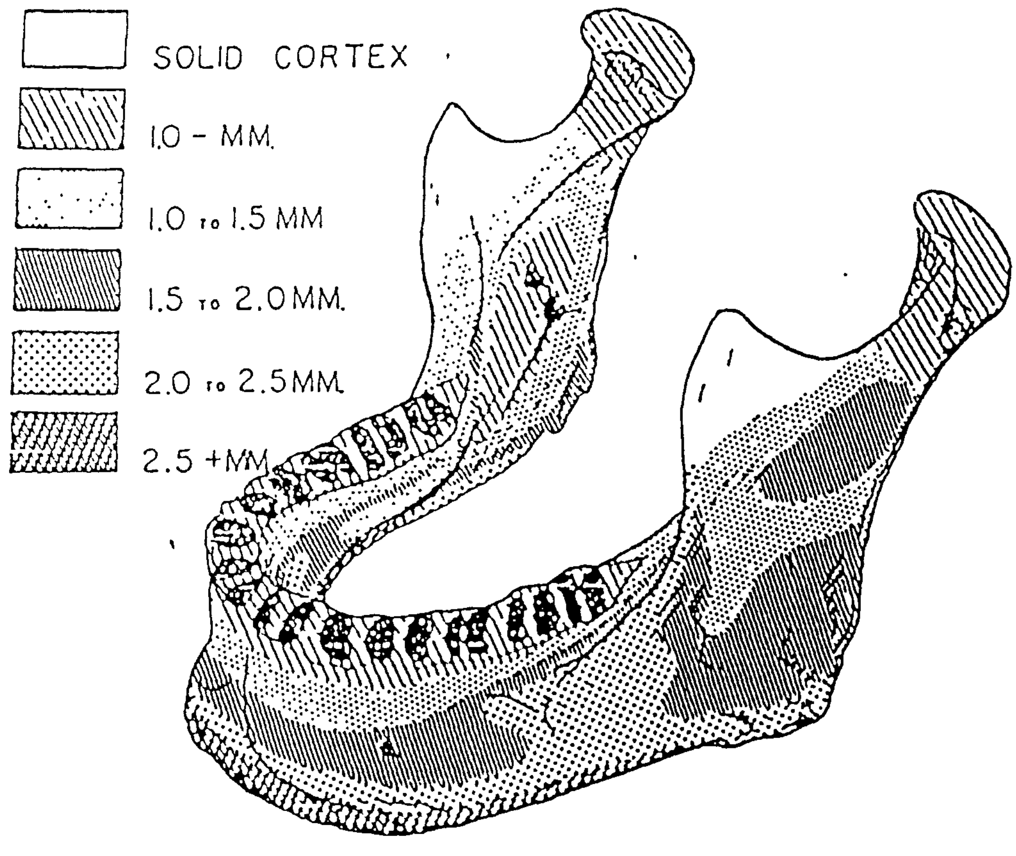

Figure 3.2 Thickness of Mandibular Cortical Bone [20]

3.2 Description of Mastication Muscles and Temporomandibular Joint

The muscles of mastication pass from the base of the skull to the mandible. These four muscles are the temporalis, masseter, and medial and lateral pterygoids [21, 22, 23, 24] (see Figure 3.3, 3.4, 3.5).

The temporalis and masseter muscles are situated on the lateral surface of the skull, partly under cover of muscles of the facial group. The temporalis muscle, which resembles the quadrant of a circle, arises from the temporal fossa and is inserted into the coronoid process of mandible; the thick, quadrilateral masseter muscle arises from the zygomatic arch and is inserted into the lateral surface of the ramus and angle of the mandible. The pterygoids are more deeply seated. The cone-shaped lateral pterygoid arises from the lateral side of the pterygoid process and lower surface of the great wing of the sphenoid and is inserted into the pterygoid fovea of the mandible and the capsule of the joint. The thick, quadrilateral medial pterygoid parallels the masseter. It arises from the pterygoid fossa of the sphenoid and is inserted into the inner side of the mandible.

The movements permitted by the temporo-mandibular joint are depression (opening) and elevation (closing), protraction (drawing forward) and retraction (drawing backward), and rotation (side-to-side movement) of the jaw. Slight hinge movements, as during ordinary conversation, occur in the lower compartment between the condyle and the disk. During wider opening of the jaw, the condyle turns hingelike of the articular disk while at the same time the disk, together with the condyle, glides forward so as to rise upon the articular tubercle. The axis for this movement is transverse through the lower third of the ramus of the mandible. The axis is not stationary but describes an ellipse during the movement.

Protraction and retraction are primarily gliding movements between the articular disk and the articular tubercle. Rotation at the temporomandibular joint, which provides the side-to-side motion, occurs alternately around a vertical axis through the neck of the mandible. This axis is through the condyle on the side toward which rotation occurs. The excursions of the condyles during the protraction and retraction and during the rotation can also be readily palpated. The fibers of the temporal, masseter, and medial pterygoid muscles are primarily vertical and therefore elevate the jaw. The fibers of the pterygoid muscles, particularly the lateral pterygoid, arise anterior and medial to the condyles of the mandible and therefore rotate the point of the jaw to the opposite side and produce grinding movements by contracting alternately on the rought and left sides.

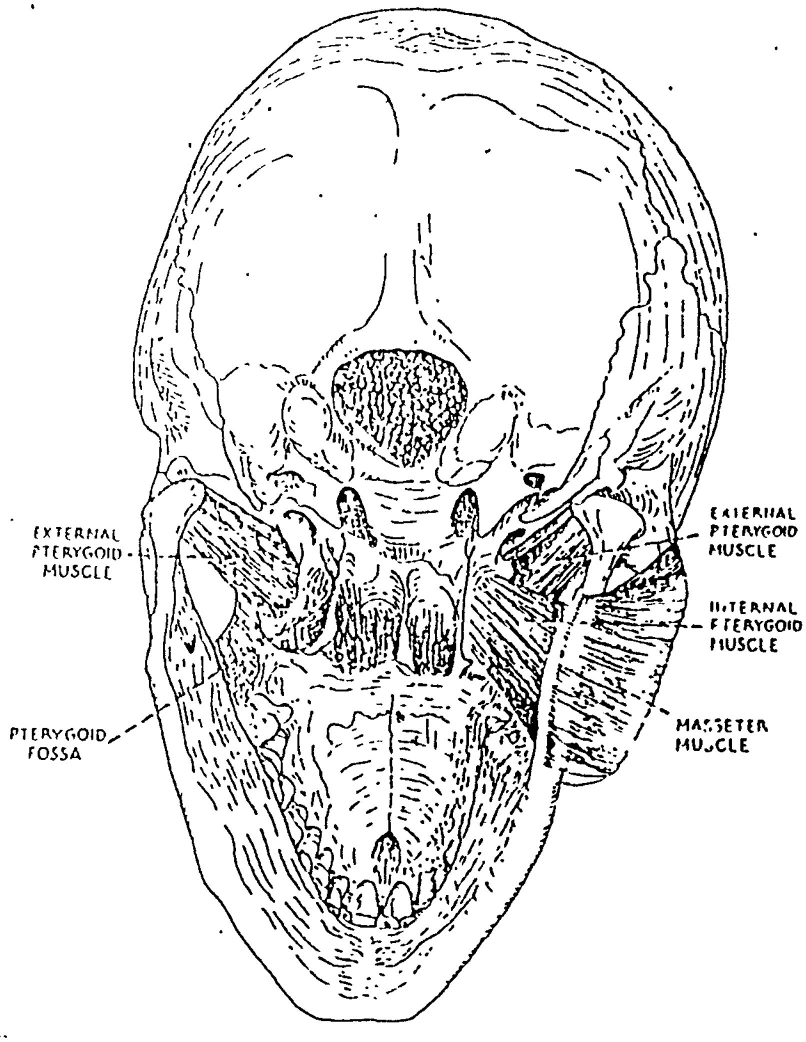

Figure 3.3 The Internal and External Pterygoid Muscles seen from behind and beneath [22]

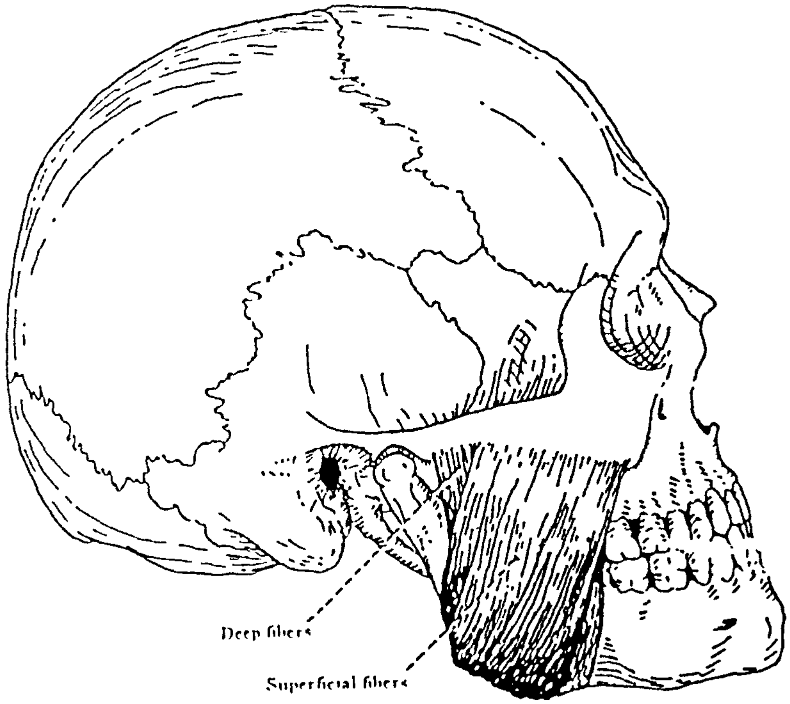

Figure 3.4 The Masseter Muscle [22]

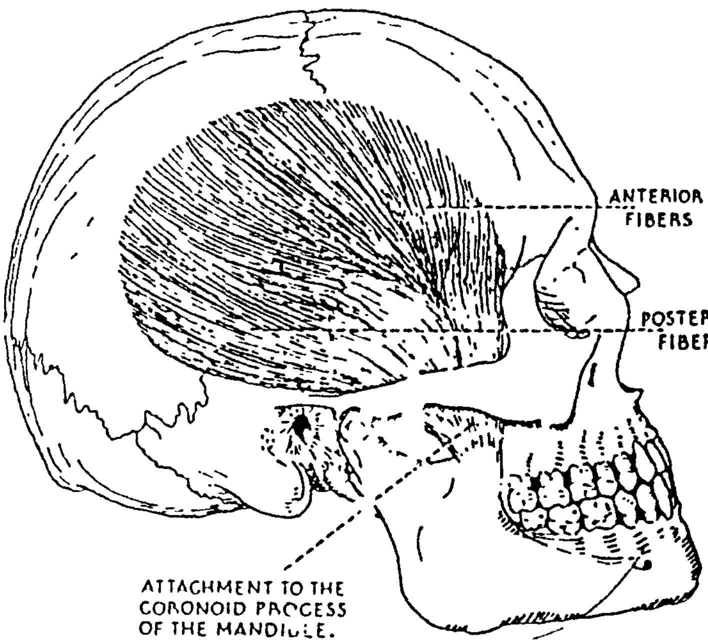

Figure 3.5 The Temporalis Muscle [22]

Chapter 4
Introduction to Finite Element Analysis in I-DEAS V

4.1 Introduction to I-DEAS V

I-DEAS[TM] (Integrated Design Engineering Analysis Software) is an integrated package of mechanical engineering software tools, which is developed by SDRC (Structural Dynamics Research Corporaton). The purpose of this software is to facilitate a concurrent engineering approach to mechanical engineering product design and analysis. The I-DEAS is made up from a number of "Families" of software modules, each subdivided further in "Task", all executed from a common menu and sharing a common database. The main families are:

Solid Modeling

Drafting

Finite Element Modeling and Analysis

System Dynamics

Test Data Analysis

Manufacturing

In this study the I-DEAS command was shown as it was shown in the menu guide.

4.2 Introduction to Finite Element Model and Analysis

Finite Element Analysis (FEA) [18] is a process which predicts deflections and other effects of stress on a structure. Finite Element Modeling (FEM) divides the structure into a grid of "elements" which form a model of the real structure. Each of the elements is a simple shape (such as a square or a triangle) for which the element program has information to write the governing equations in the form of a stiffness matrix (see appendix 3 for stiffness matrix). The unknowns for each element are the displacements at the "node" points, which are the points at which the elements are connected. The finite element program will assemble the stiffness matrix for these simple elements together to form the global stiffness matrix for the entire model. This stiffness matrix is solved for the unknown displacements, given the known forces, material properties and boundary conditions. From the displacements at the nodes, the stresses in each element can then be calculated.

A finite element is derived by assuming an equation for the internal strain. Some elements are defined to assume that the strain is constant throughout the element, while others use higher-order functions. Using these equations between the external forces and the nodal displacements can be written as Huke formula.

$$f_i = k_i d_i$$

where f_i is the element applied force, d_i is the element displacement and k_i is the Huke coefficient.

There will be one equation for each degree of freedom for each node of the element. These equations are most conveniently written in matrix form for use in a computer algorithm. The matrix of the coefficients k_i becomes a "stiffness matrix" **[K]*** that relates forces to displacements.

$$\{\mathbf{F}\}=[\mathbf{K}]^*\{\mathbf{d}\}$$

where **[K]** is the stiffness matrix and **{d}** is the displacement matrix.

Even though the unknowns are at discrete degrees of freedom, the internal equations are written for strain functions that represent a continuum. This means that even though the finite element model has a discrete number of equations. If the correct elements are chosen, it is possible to converge on a correct answer with a less-than-infinite number of nodes and elements.

A finite element model is the complete idealization of the entire structural problem, including the node location elements, physical and material properties, loads and boundary conditions. The model will be defined differently for different types of analysis: static structural loads, dynamics, or thermal analysis.

A finite element model is often made of more than one element type. The finite element model is constructed to mathematically model the deflection of the structure, not to look like it. Parts of a structure might be best modeled with beam elements, and other parts with thin shell elements.

The accuracy of the resulting solution will depend on how well the structure was modeled, the assumptions made for loads and boundary conditions, and the accuracy of the elements used for the given problem. In general, the solution will be more accurate as the structure is subdivided into smaller elements. The only sure way to know if there is a sufficiently converged on the final solution is to make more models with finer grids of elements and check the convergence of the solution.

The purpose of finite element modeling is to make a model that behaves mathematically like the structure modeled, not necessarily the one that looks like the real structure.

4.3 Steps in Finite Element Analysis of I-Deas V

The family of Finite Element consists of three steps. These are:

1) Pre-Processing

Mesh Creation Task

Geometry Modeling Task

Boundary Condition Task

2) Solution

Model Solution Task

3) Post-Processing

Post Processing Task

Pre-processing includes the entire process of developing the geometry of a finite element model, entering physical and material properties, describing the boundary conditions and structural loads, and checking the model.

The Solution phase can be performed in the Model Solution Task of I-DEAS Finite Element Modeling & Analysis, or in an external finite element analysis program. I-DEAS Model Solution can solve linear statics, linear dynamics, conduction heat transfer, and potential flow analysis. For other types of analysis such as non-linear statics, the finite element model information can be wr[illegible] the format required for an external finite element solver such as ANSYS.

Post-processing involves plotting deflections and stresses, and comparing these results with failure criteria imposed on the design such as maximum deflection allowed, the material static and fatigue strengths, etc. Because of the complicated composition of mandibular bone, the criteria was not used in this study. Post-processing also involves checking for errors that might not have been detected while building the model. Furthermore, Post-processing involves refining the mesh depending on the solutions which are produced by the previous mesh creation.

Chapter 5
Boundary Conditions

5.1 Mastication Muscles and Its Force Estimation

The human mastication system consists of upper and lower jaw, connected by two temporomandibular joints and by four pairs of muscles, that have a capacity to close the jaw. Each muscle can generate a force vector with a specific spatial orientation. Different combinations of action of the mastication muscle results in both the different magnitude and direction.

According to Weijs *et al,* the maximum muscle force of a muscle element is assumed to be proportional to its physiological cross section (PCS) under static circumstances [5] . This is expressed by

$$F_{i,max} = P \times A_i \tag{5.1}$$

where P is a constant called intrinsic strength, $P = 0.37 \times 10^6 Nm^{-2}$ and A_i is the PCS of muscle element i. Using the data obtained by Weijs [5], the maximum muscle forces were obtained (see Table 1, column 1).

Osborn [25] used another data group of maximum force of mastication muscle when he tried to establish a predicted pattern of human mastication system muscle activity (see Table 1, column 2).

Koolstra, *et al* [7] used MRI to measure the both side muscle PCS of seven healthy male subjects. Choosing the same intrinsic strength: $P = 0.37 \times 10^6 Nm^{-2}$ and averaging the data the authors obtained, the average PCS and corresponding average maximum force were shown in Table 1, column 3. The forces were expressed in Newton.*

*for unit conversions,

$$1N = \frac{1}{4.448} lb, \qquad \text{and} \qquad 1Pa = \frac{1}{6894.8} psi$$

Table 1: The Maximum Forces (N) of Mastication System Muscles Obtained by Weijs, Osborn and Koolstra

Muscles element	Weijs	Osborn	Koolstra
Masseter muscle, superficial part Masseter muscle, deep part	210.9 85.1	450.8	334.48
Medial pterygoid muscle	162.8	254.8	201.28
Lateral pterygoid superior head Lateral pterygoid muscle inferior head	29.6 51.8	382.2	36.26 83.99
Temporalis muscle anterior part Temporalis muscle posterior part Temporalis muscle deep part	129.5 166.5 40.7	264.6 323.4	217.93 180.93
Digastric		107.8	

Combining the data obtained by three authors above, the force of the mastication system muscles for the study was obtained (see Table 2). The effection of digastric muscle was ignored in static situation.

Table 2: Mastication System Muscle Force Used as Restrain Force in Finite Element Analysis Model

Muscle element	Force(N)
Masseter muscle	315.24
Medial pterygoid muscle	182.04
Lateral pterygoid muscle	100.83
Anterior temporalis muscle	183.8
Posterior Temporalis muscle	183.7

5.2 The Constraint of Temporo-mandibular Joint

In 1975, Hylander [26] discussed the temporo-mandible joint (TMJ) in his dissertation. He concluded that in the static situation the TMJ is a link and in the dynamic situation the

TMJ is a lever. Therefore the link theory [32]was used as the constraint since this study only discusses the static and linear situation.

5.3 Structural Load and Additional Contraint

A compressive structural load was applied to the midline of the mandible in x-axis direction to simulate the trauma caused by an impact automible accident. According to I-DEAS's coordinate definition, x-axis is the depth in the saggital plane, y-axis is the height in the saggital plane and z-axis is the width in the transverse plane (see appendix 1). For high resolution of stress distribution, 1,500N (337 lb) was chosen as the structural load. Because the second molar area is very close to the skull, it is assumed that the area is fixed.

5.4 The Demonstration of Boundary Condition and Structural Load

In this study, the boundary condition was similar to one used by Umetani [10]. Considering the anatomic characteristics of pterygoid muscles and masseter muscle, however, the direction of muscle force applied on the mandibular angle was changed as 15° from y-axis (see Figure 5.1 and Figure 5.2). The mastication system muscle forces were chosen as the average of which found from several other articles [11, 12, 5, 7, 25] (see Table 2).

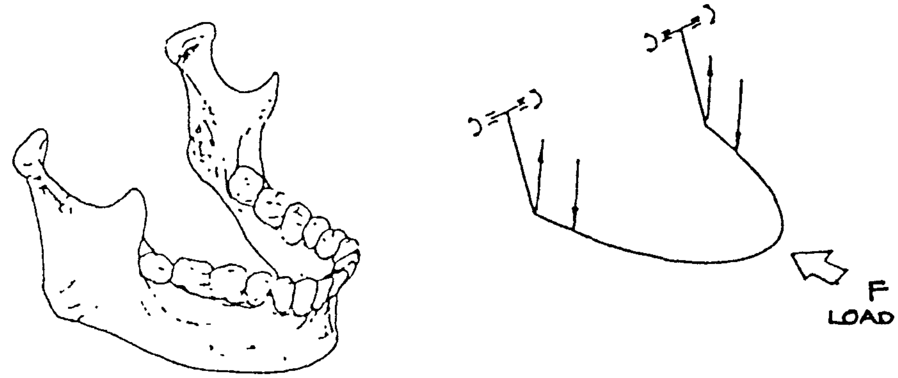

Figure 5.1 Simplified Modeling of Mandible [10]

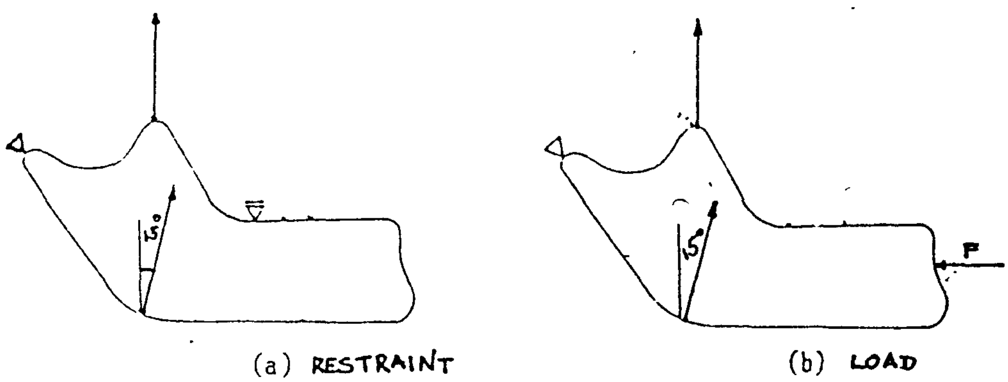

Figure 5.2 Boundary Condition of Mandibular Bone [10]

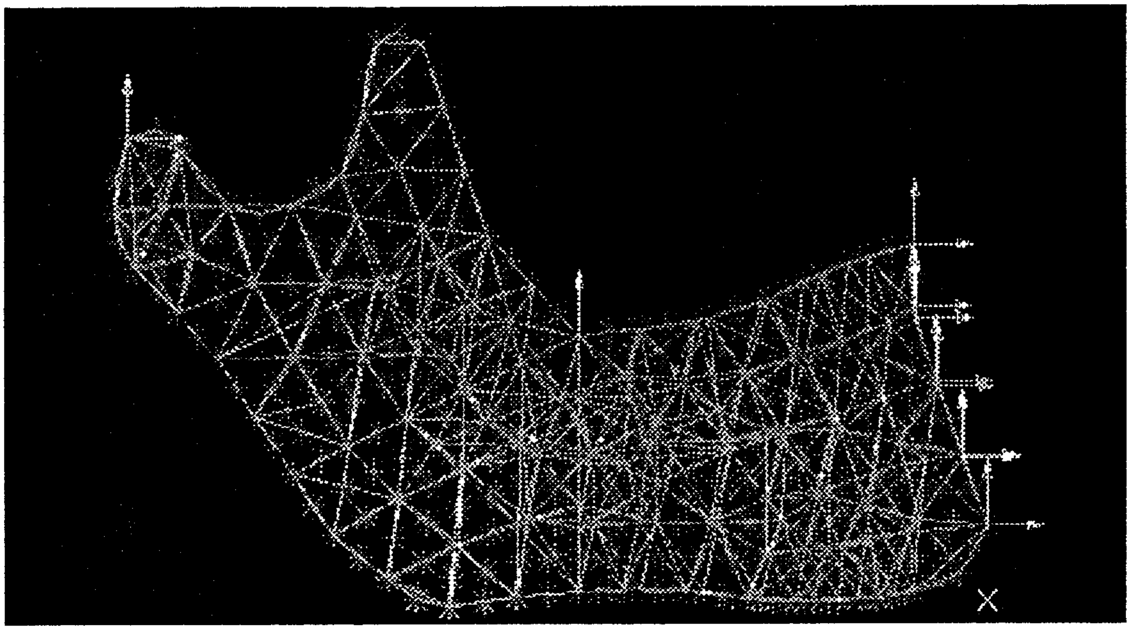

Figure 5.3a. Restraints Used in the Study Shown by I-DEAS

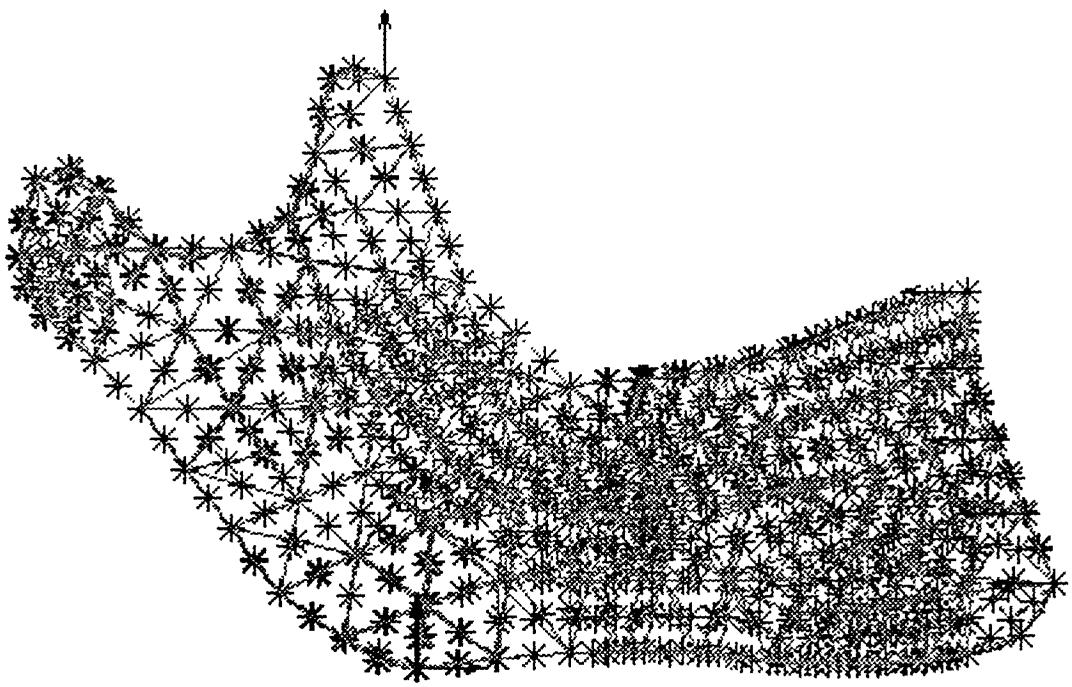

Figure 5.3 b. Structural Load and Muscle Forces Used in the Study Shown by I-DEAS

It were presented how the I-DEAS shows the restraints and structural load on the mandible model (see Figure 5.3 a, b). The condyle process was treated as a hinge, which with rotation freedom but without displacement freedom. The area of the second molar was assumed that there is no deformation in the positive y-axis direction, and that the midline of the mandible was fixed in the z-axis due to the axi-symmetric constraint condition of finite element analysis (see Figure 5.3 a).

The temporal muscle force was shown in the coronoid process in y-axis direction. The forces of the masseter muscle and the pterygoid muscle were shown as two directional forces. Their resultant force is 15° from y-axis. These forces of mastication system muscles are the portion of the support (i.e. the restraint force) of the mandible. The only applied load is the compressive force (with the arrow toward the mandible) along the midline of the mandible (see Figure 5.3 b).

All the restraints were expressed by arrows. In I-DEAS, it is not necessary that an arrow represents a force. The arrow is also used to express the other boundary conditions, such as freedom limitation of deformation or movement. After the boundary conditions and the structural load were all applied on the model, in some areas the arrows represent the restraint might be coincident with the one represents the structural laod. Therefore, it must be very careful when the boundary conditions and the structural load of the model were modified.

Chapter 6
Method and Material

6.1 Method

6.1.1 Model Establishment

Using the optical comparator to measure a mandible bone, 64 data points on half of the mandible were obtained (see Figure 6.2). That is from the symphysis to the end of the condyle (see appendix 1). By using the I-Deas V software program language (see appendix 2), a three dimensional model of mandible bone was established by line and spline (see Fig 6.1 a-d).

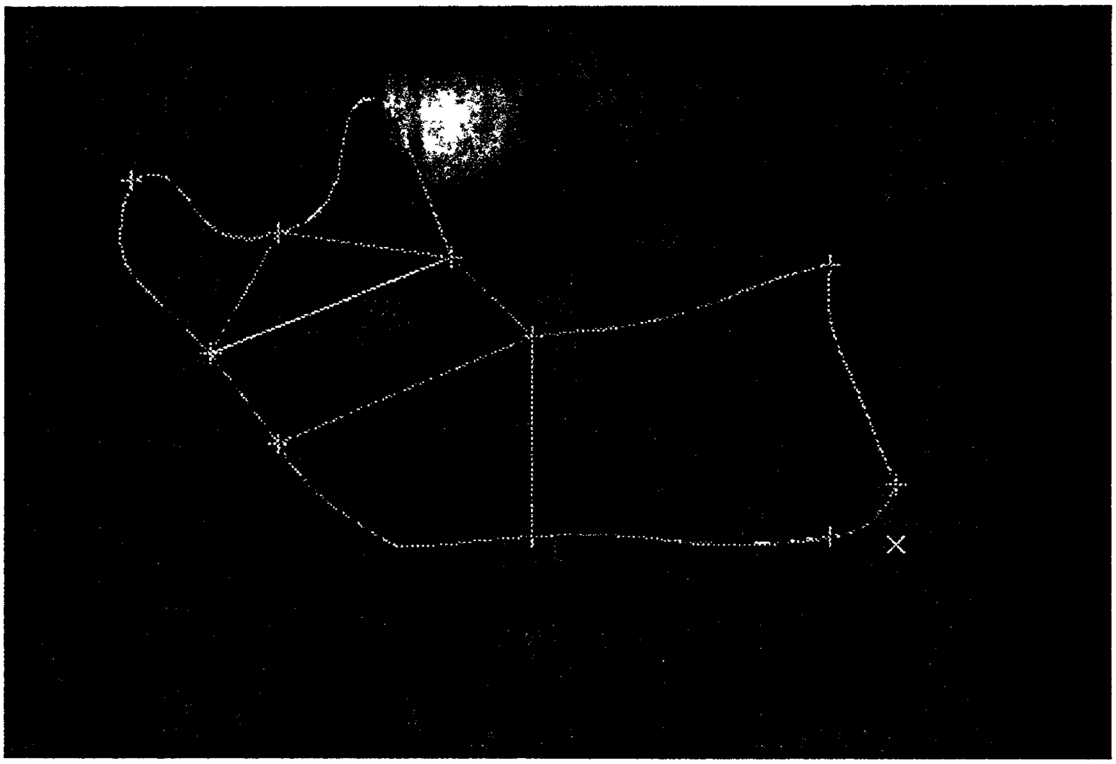

Figure 6.1 Mandible Model Established by Using I-DEAS V
a. lateral view

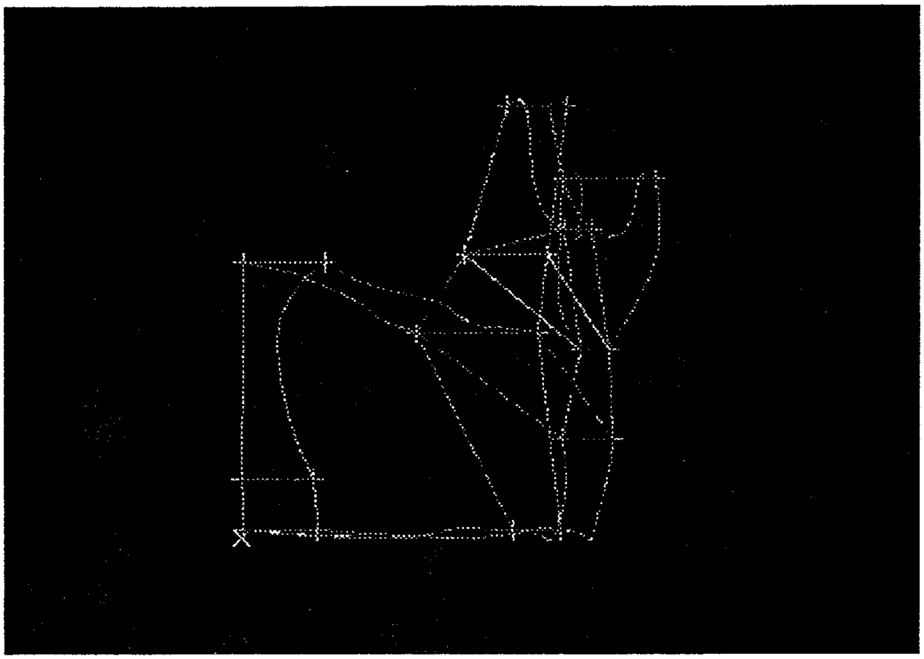

Figure 6.1 Mandible Model Established by Using I-DEAS V
b. frontal view

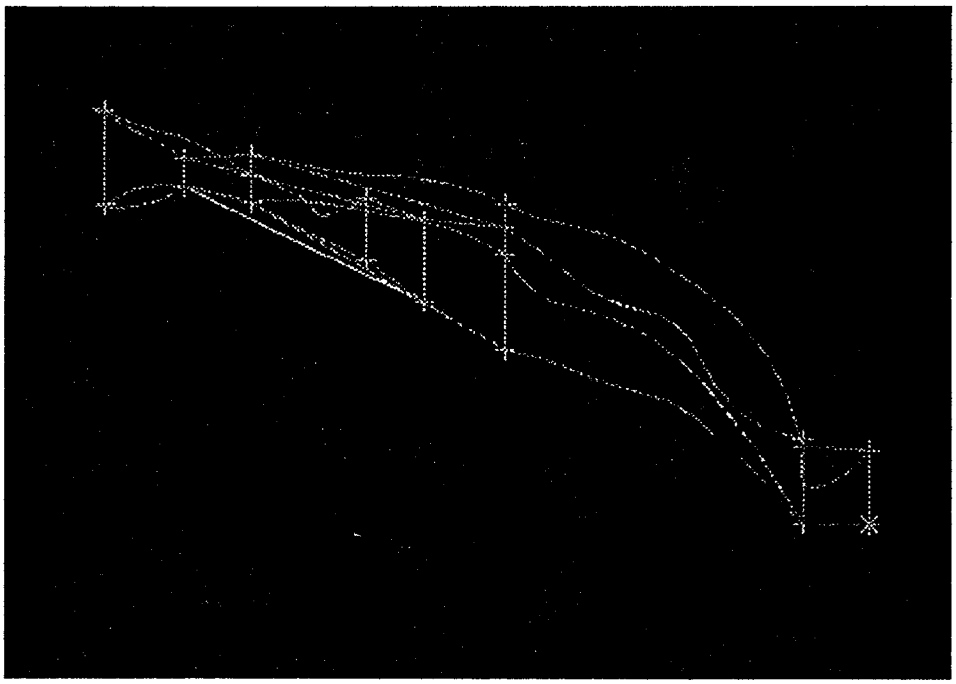

Figure 6.1 Mandible Model Established by Using I-DEAS V
c. top view

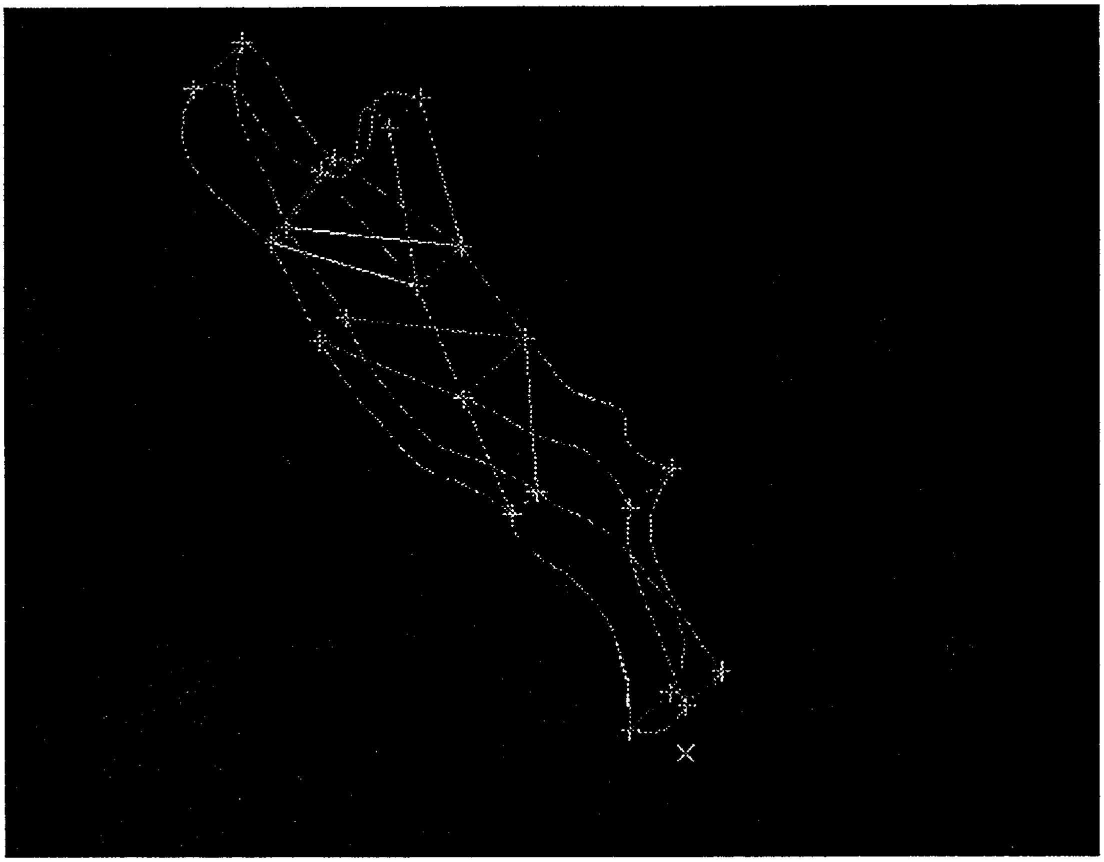

Figure 6.1 Mandible Model Established by Using I-DEAS V
d. isometric view

Because the mandible is symmetrical about the saggital plane, a model of half of the mandible is needed to study its mechanical property by using the finite element analysis method [27]. According to the traditional description of the mandible [28], the mandible was divided into several areas: mandible body, mandible angle, mandible ramus, condyloid process area and coronoid process area. (see Figure 7.1).

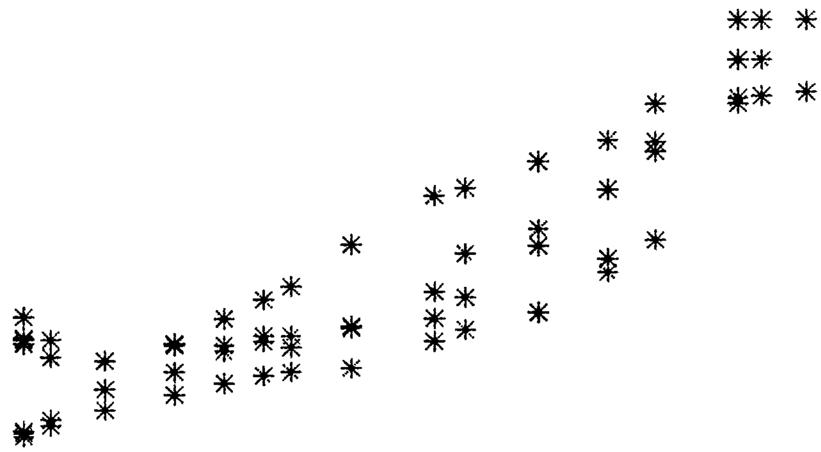

a) the top view

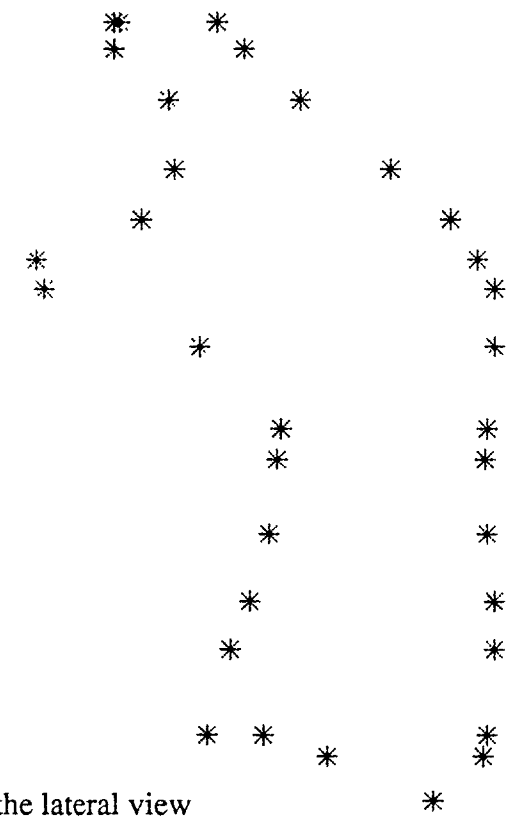

b) the lateral view

Figure 6.2 The 64 Points of the Mandible Obtained by Optical Comparator

From the four figures with different viewing directions the following conclusions were drawn:

1. Although the model is an approximate model, it represents most of the characteristics of the mandible. It could be used as a model of mechanic analysis.

2. It does not reflect the details of mandible anatomy characteristics, since using the optical comparator could not give a detailed description as the CT scan. Because the CT scan data directly loaded to I-DEAS are not available in this study because of the limitation of technique, time and finance.

3. By the same reason as 2. , the model does not very well simulate the real condyle and the all edges of the mandible.

4. Compared with some articles [9, 14] using more than thousands elements to study a mandible model with teeth, this model could still provide a simplified and effective understanding of the mandible, the stress distribution could be used to compare with the clinical investigation.

6.1.2 Create Mesh

Under the Finite Element Modeling &Analysis Family in I-DEAS V, the mesh creation task automatically generated a free mapped mesh. The total number of elements generated is 487 element (see Figure 6.3). Because of the memory limitation of the Sun workstation, more elements could not be analyzed. It takes almost an hour to run the solution in I-DEAS. It also takes 76% of CPU time and 71% of memory of Sun workstation at the peak during the solution being operated. The command is:

Mesh Creation

Mesh_Volumes

Mesh_Size

Mesh Generate

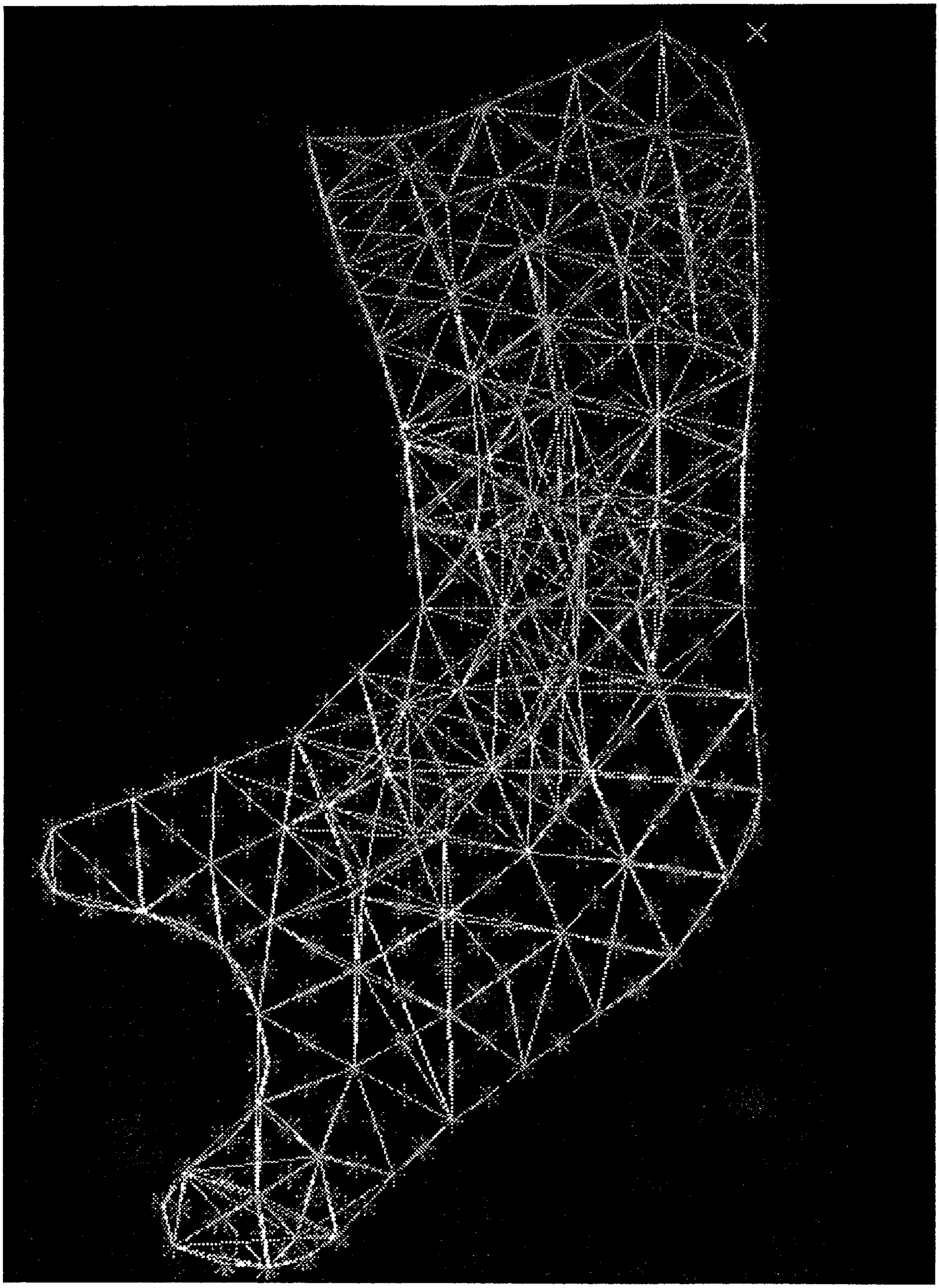

Figure 6.3 Three Dimension Mandible Model Meshed With 487 Elements (lateral view)

A difficult problem is how to define the mesh volumes. The Geometry Modeling Task in the Finite Element Modeling & Analysis Family is much less flexible and powerful than the one in Solid Modeling Family.

As a regular shape, such as block, sphere, cylinder, cone etc. in the Geometry Modeling task under Solid Modeling, the model can be manipulated widely by the command such as "round the edges", "reflect the graph", or turn the solid model into finite element model through the Surface/Solid command in Finite Element Modeling & Analysis Family.

Since the mandible has an irregular shape, the model was created depending on the discrete data points by Spline and Line under the Mesh Creation Task. After the screen model was established, the volumes of model had to be defined for the program to recognize the screen model as a defined geometry model.

In Mesh Generate Task, it was possible to choose the type of and size of element. In this study, the element was chosen as tetra (see appendix 3), free mapped, and the size-length of element is 0.3 fold of the size-length of the area defined. For more accurate results, the mandible was divided into several areas (see Figure 6.1 a) depending on the previous computer model and calculation. Using this technique, the program automatically generated a total number of 487 elements mesh to be used for the study.

I-DEAS also has several interfaces with other finite element analysis program such as ANSYS. When the mesh is generated and boundary conditions applied, the file can be written into ANSYS file format or Universal file format and transfer to ANSYS to run the data. The output data can be picked back by I-DEAS through Post Process Task in I-DEAS. In this study, the ANSYS was often used to run some intermediate test model. The results were used as parameters to setup more effecient models and meshes in I-DEAS. Because of its faster calculation speed, for same amount of elements it is four times faster than I-DEAS.

6.1.3 Boundary Condition

After the establishment of the model mesh, the Boundary_Condition Task can be used to apply the restraint and the force. The command is :

Boundary_Condition

Restraint

Structural Load

For restraint, it had to apply not only the restraint of the problem, but also the symphysis restraint of finite element method since only half of the mandible was studied. In I-DEAS all the forces are applied in the menu of Structural_Load, no matter whether it is the restraint force or the structural load.

6.1.4 Solution

After the establishment of the model mesh and the application of boundary conditions, the Model_Solution Task can be used to calculate the displacement and the stress distribution. The command is:

Model_Solution

Output_Selection

Solve_Linear_Statics

Report_Solution_Errors

It is very important to have the program report the solution errors. The model is checked for convergence and well established, which includes mesh creation, application of boundary condition and establishment of model. I-DEAS will report errors including twisting elements, missing or repeated mesh and other kind of errors. This feature is the most powerful and popular feature of the advanced computer aid design program as mentioned in Chapter 2.

If there are some errors reported one has to go back to the task of Mesh Generation, Boundary Condition or Geometry Modeling where the error ever occurred. Otherwise, one may continue the operation to Post Process.

6.1.5 Post Process

I-DEAS Post Process Task provides a wide selections of output demonstration and input ability (it can input the results from MSC/NASTRAN, COMIC_NASTRA, ANSYS, and ABAQUS). In this study, deformed geometry and maximum principal stresses were obtained (see figures in Chapter 7).

The command is:

Post_Process.

Group

Analysis_Dataset_Set

Manage_Models

In Post Process, the output functions depend on the function of Display_Option command. In I-DEAS, the Display_Option command in the main menu comes with each Task, thus I-DEAS has a powerful graphic function. The graph can be displayed in maximum 15 different colors and 4 outlay selections.

6.2 Material Property

Due to the complicated shape and structure of the mandibular bone, there are only several studies which focused on the study of elastic constants. Depending on the data obtained by Ashman [11], the following constants were chosen as the mandible cortex mechanical property (see Table 5).

Table 3: Elastic Constants of Mandible Cortex

Elastic constants	value
Young Modulus	2.7Mpsi
Possion ratio	0.32

Due to the limitation of the simulation technique, it was omitted the factor that the cancellous bone exerts a lot influence on the whole bone structure [29, 30]. For the same technical reason it was assumed that the mandible is isotropic and homogeneous.

Once the material properties were chosen, one can go back to the Mesh_Creation Task to modify the material properties which are provided by program. The command is:

Mesh_Creation

Modify

Material Property

For the whole procedure to establish the model and solve the problem, the menu used was expressed in appendix 5.

Chapter 7
Results and Discussion

7.1 Results

7.1.1 Contour Output

In the Post Process Task, by using the commands:

Analysis_Dataset

Current

Contour

By choosing the displacement and maximum principal stress as output data components, the color pictures were obtained (see Figure 7.2 and Figure 7.3). In I-DEAS, the contour method indicates the output data in different colors according to different ranges of output data. Usually the red color represents the largest value and the blue one represents the lowest. By contour method, one could easy decide where there are a high stress concentrations and the maximum displacement. However, this only gives a qualitative description of stress distribution and displacement distributions. The analysis of stress and displacement was focused on six areas of the mandible (see Figure 7.1 for more detail).

7.2.2 Plot Output

By defining the x-axis as node relative distance (inch), and y-axis as displacement (inch) and maximum principal stress (psi) separately, the displacement and maximum principal stress distribution were obtained. The areas which need more details to be chosen. These are: (1) coronoid process area, (2) the connection of body and ramus, (3) symphysis, (4) angle, (5) condyle process area, and (6) mandibular notch (see Figure 7.1). A series of output plot figures were obtained (see Figure 7.4--Figure 7.9). The "global y coordinate" in the plot is I-DEAS plot sign. Its mechanics meaning could be defined as different parameters. In this study, it was defined as x-axis.

By defining the x-axis as node location (inch) from the symphysis to the condyle, and y-axis as displacement (inch) and maximum principal stress (psi) separately, the whole displacement and maximum principal stress distribution of the mandible were obtained (for detail see Figure 7.10 a, b).

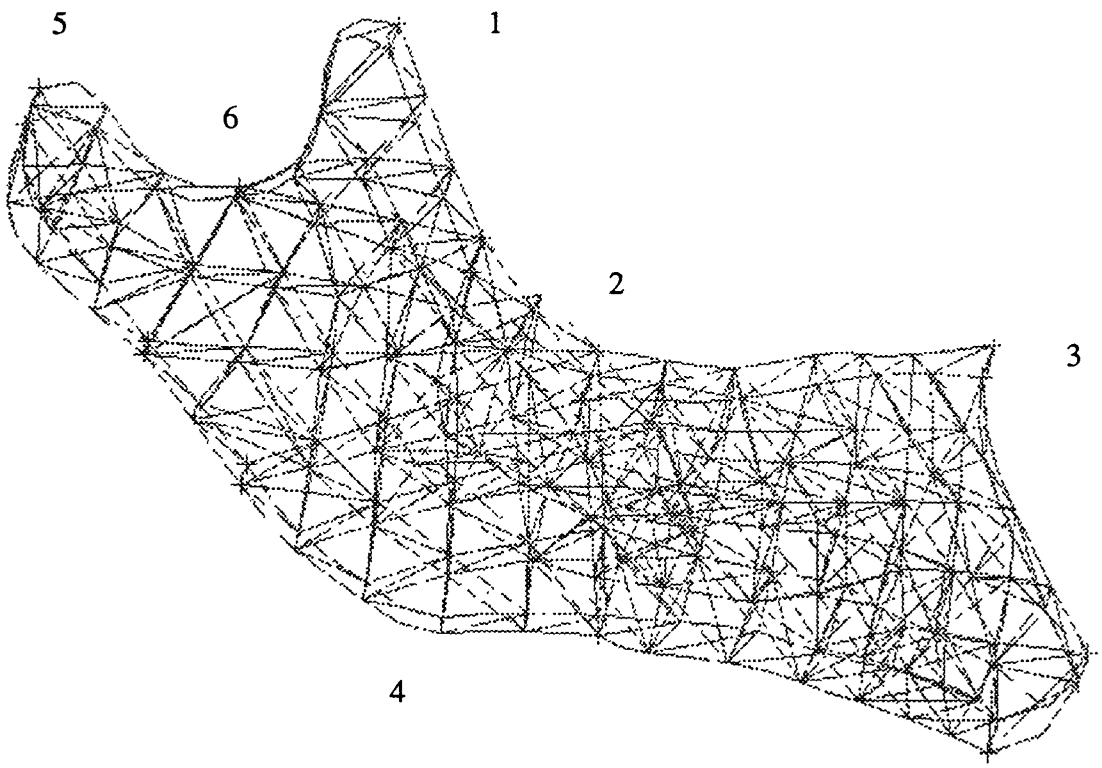

Figure 7.1 The Area Focused for Detail Plot Output

1. Coronoid Process area, 2. Connection of Body and Ramus

3. Symphysis, 4. Angle, 5. Condyle Process Area,

6. Mandibular Notch

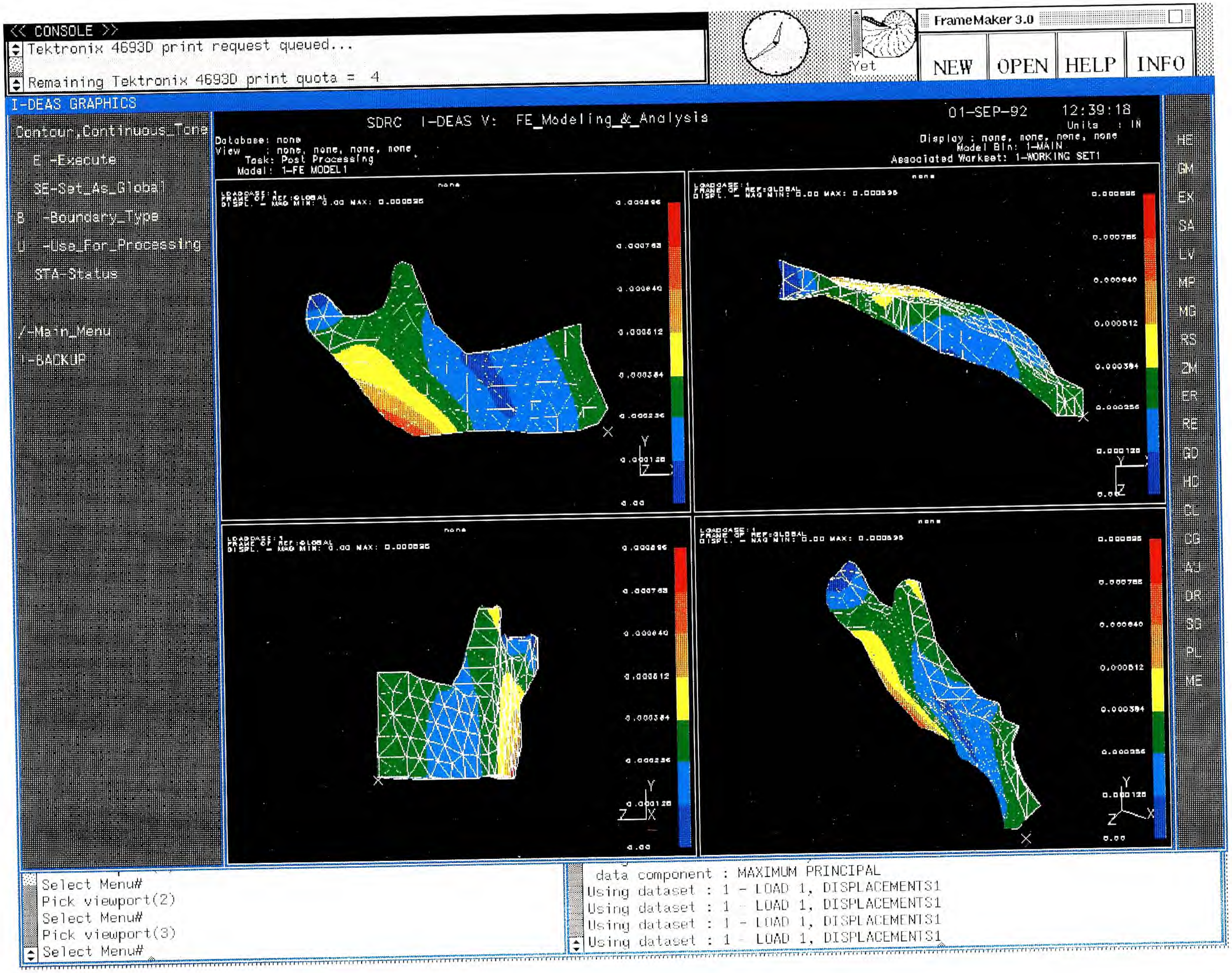
<< CONSOLE >>
Tektronix 4693D print request queued...
Remaining Tektronix 4693D print quota = 4
FrameMaker 3.0
NEW
OPEN
HELP
INFO
I-DEAS GRAPHICS
SDRC I-DEAS V: FE_Modeling_&_Analysis
01-SEP-92 12:39:18
Units : IN
Database: none
View : none, none, none, none
Task: Post Processing
Model: 1-FE MODEL1
Display : none, none, none, none
Model Bin: 1-MAIN
Associated Workset: 1-WORKING SET1
Contour,Continuous_Tone
E -Execute
SE-Set_As_Global
B -Boundary_Type
U -Use_For_Processing
STA-Status
/-Main_Menu
!-BACKUP
Select Menu#
Pick viewport(2)
Select Menu#
Pick viewport(3)
Select Menu#
data component : MAXIMUM PRINCIPAL
Using dataset : 1 - LOAD 1, DISPLACEMENTS1
Using dataset : 1 - LOAD 1, DISPLACEMENTS1
Using dataset : 1 - LOAD 1, DISPLACEMENTS1
Using dataset : 1 - LOAD 1, DISPLACEMENTS1

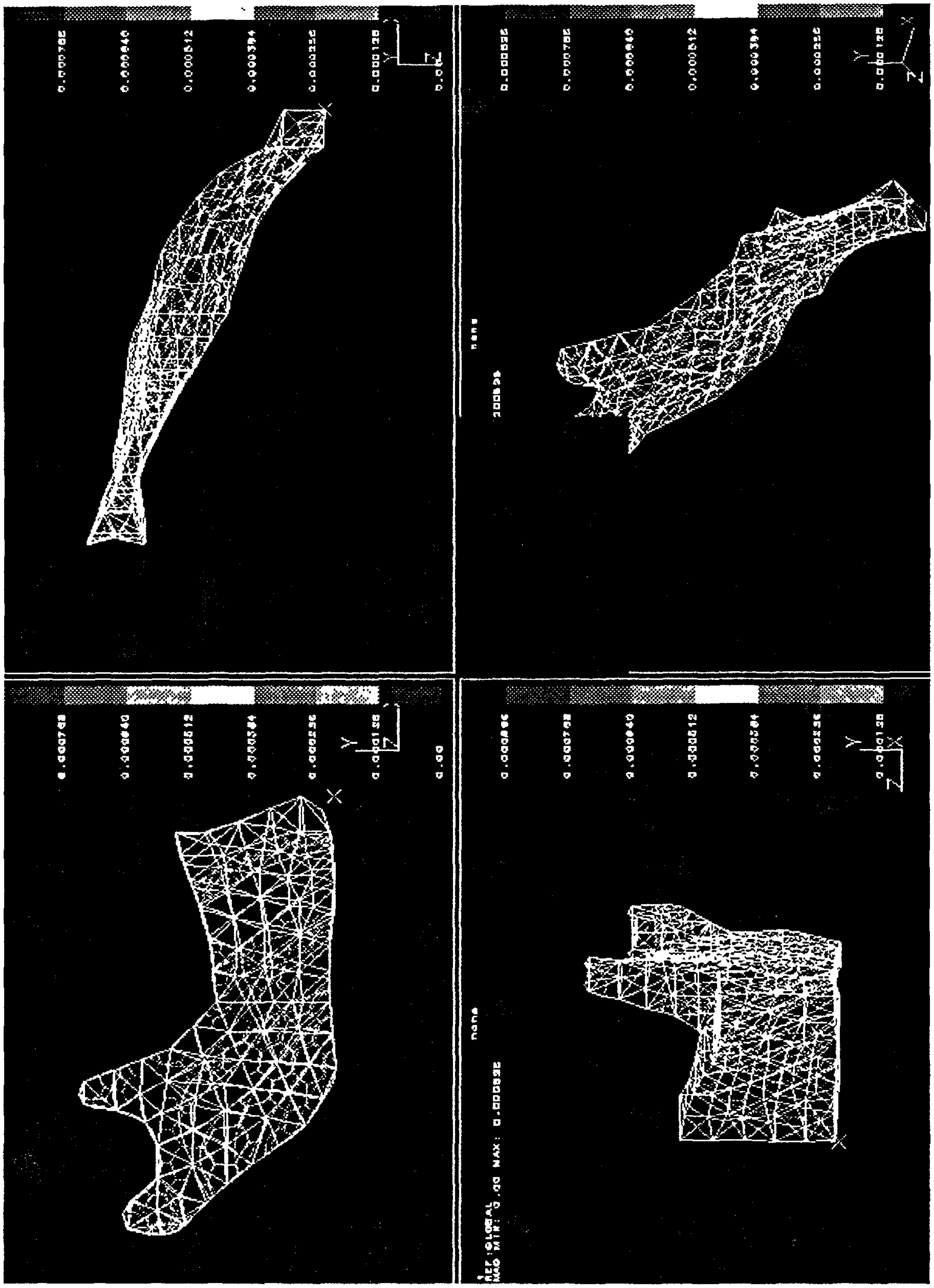

Figure 7.2 Contour Output of Displacement With Four Outlay Display

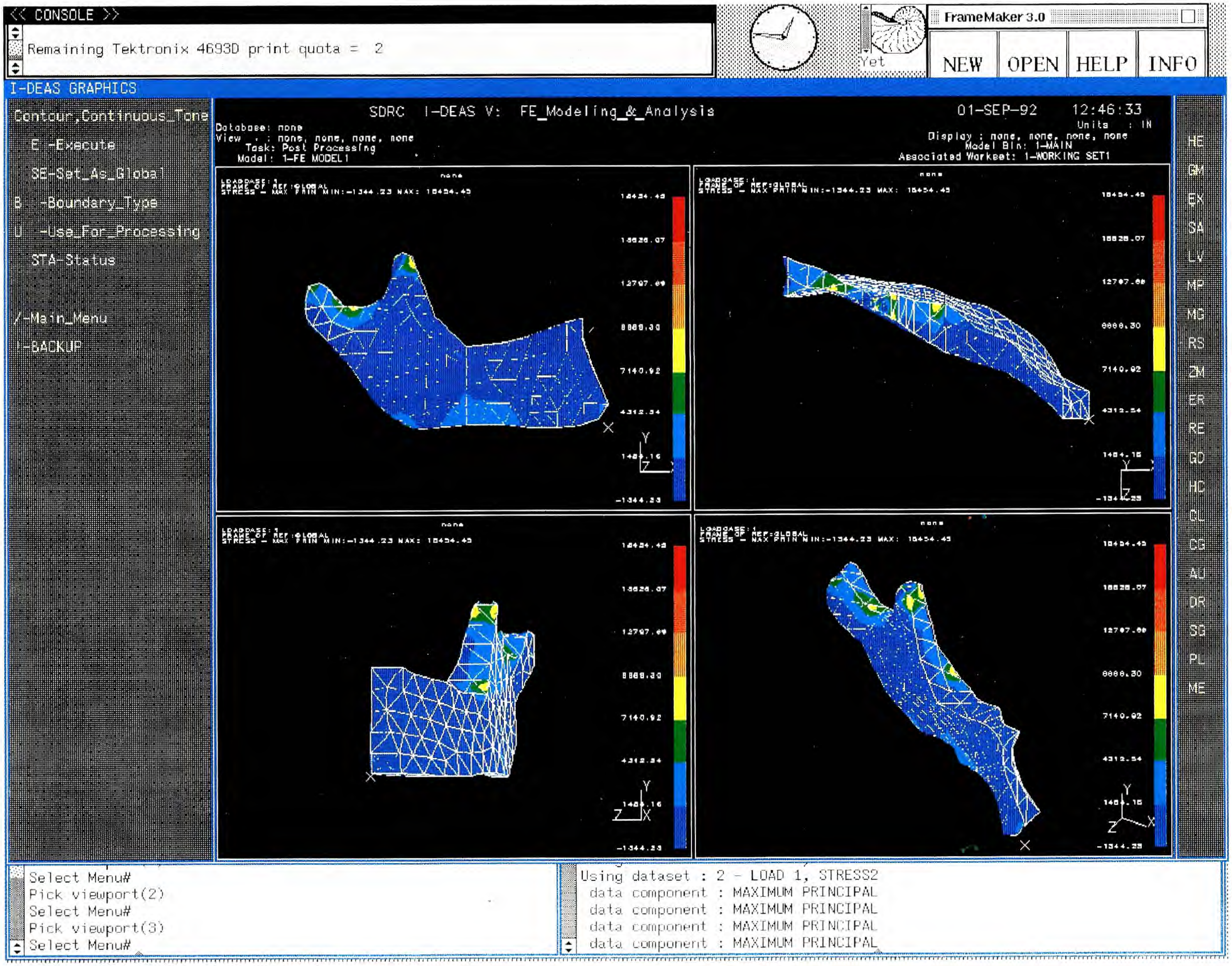

<< CONSOLE >>
Remaining Tektronix 4693D print quota = 2
FrameMaker 3.0
NEW
OPEN
HELP
INFO
I-DEAS GRAPHICS
Contour,Continuous_Tone
E -Execute
SE-Set_As_Global
B -Boundary_Type
U -Use_For_Processing
STA-Status
/-Main_Menu
!-BACKUP
SDRC I-DEAS V: FE_Modeling_&_Analysis
01-SEP-92 12:46:33
Database: none
View : none, none, none, none
Task: Post Processing
Model: 1-FE MODEL1
Units : IN
Display : none, none, none, none
Model Bin: 1-MAIN
Associated Workset: 1-WORKING SET1
HE
GM
EX
SA
LV
MP
MG
RS
2M
ER
RE
GD
HC
CL
CG
AU
DR
SG
PL
ME
Select Menu#
Pick viewport(2)
Select Menu#
Pick viewport(3)
Select Menu#
Using dataset : 2 - LOAD 1, STRESS2
data component : MAXIMUM PRINCIPAL
data component : MAXIMUM PRINCIPAL
data component : MAXIMUM PRINCIPAL
data component : MAXIMUM PRINCIPAL

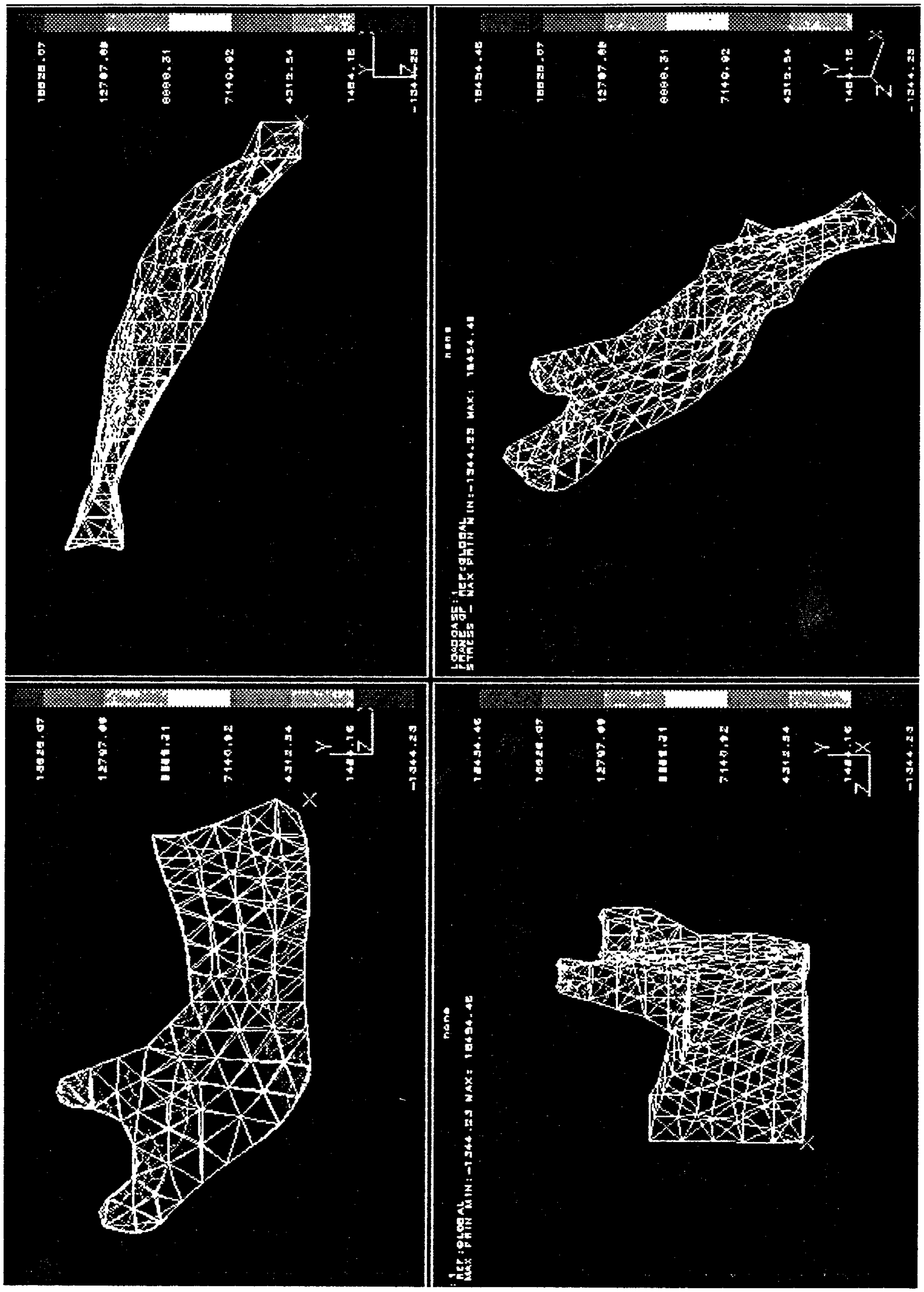

Figure 7.3 Contour Output of Maximum Principal Stress With Four Outlay Display

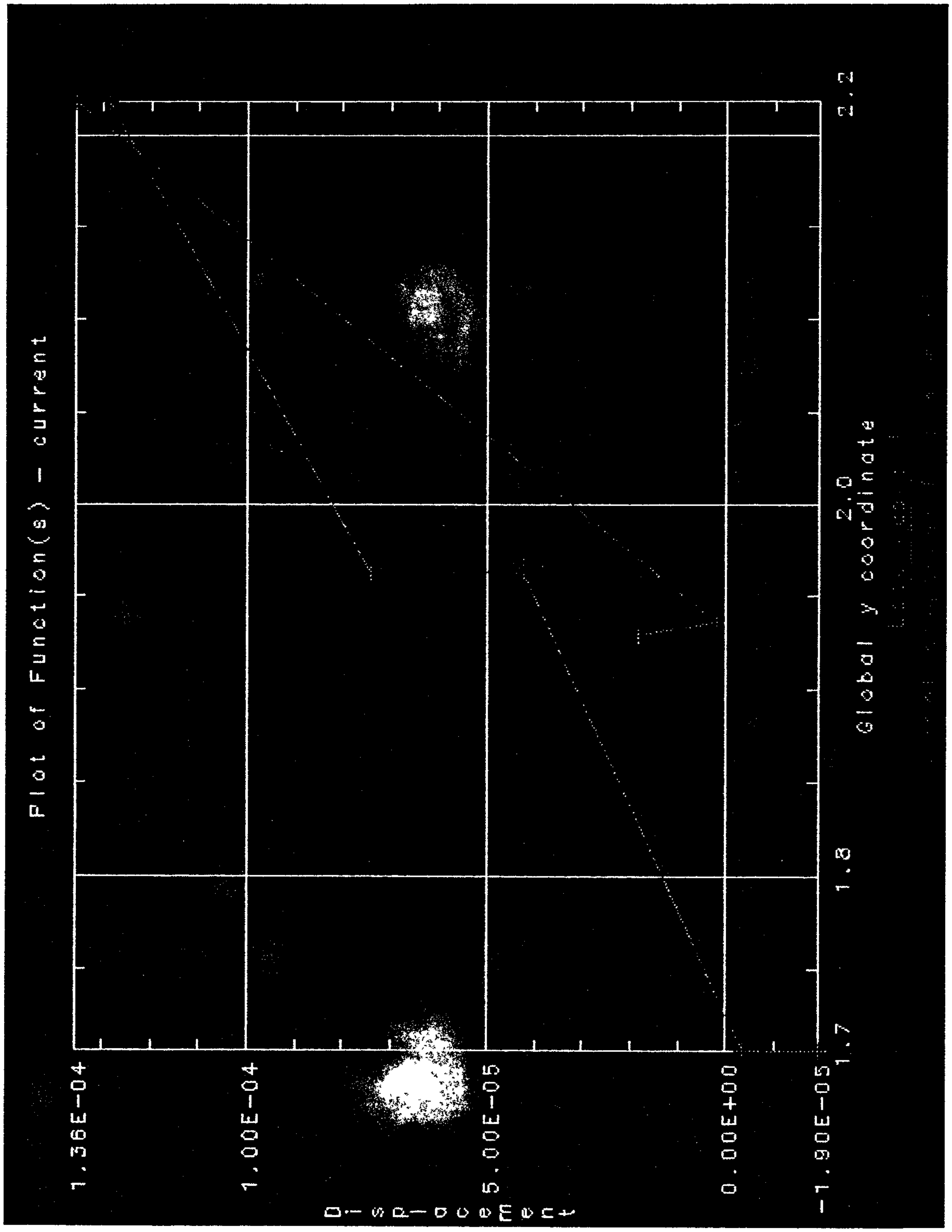

Figure 7.4 a. Displacement in the Coronoid Process Area

Figure 7.4 b. Maximum Principal Stress in Coronoid Process Area

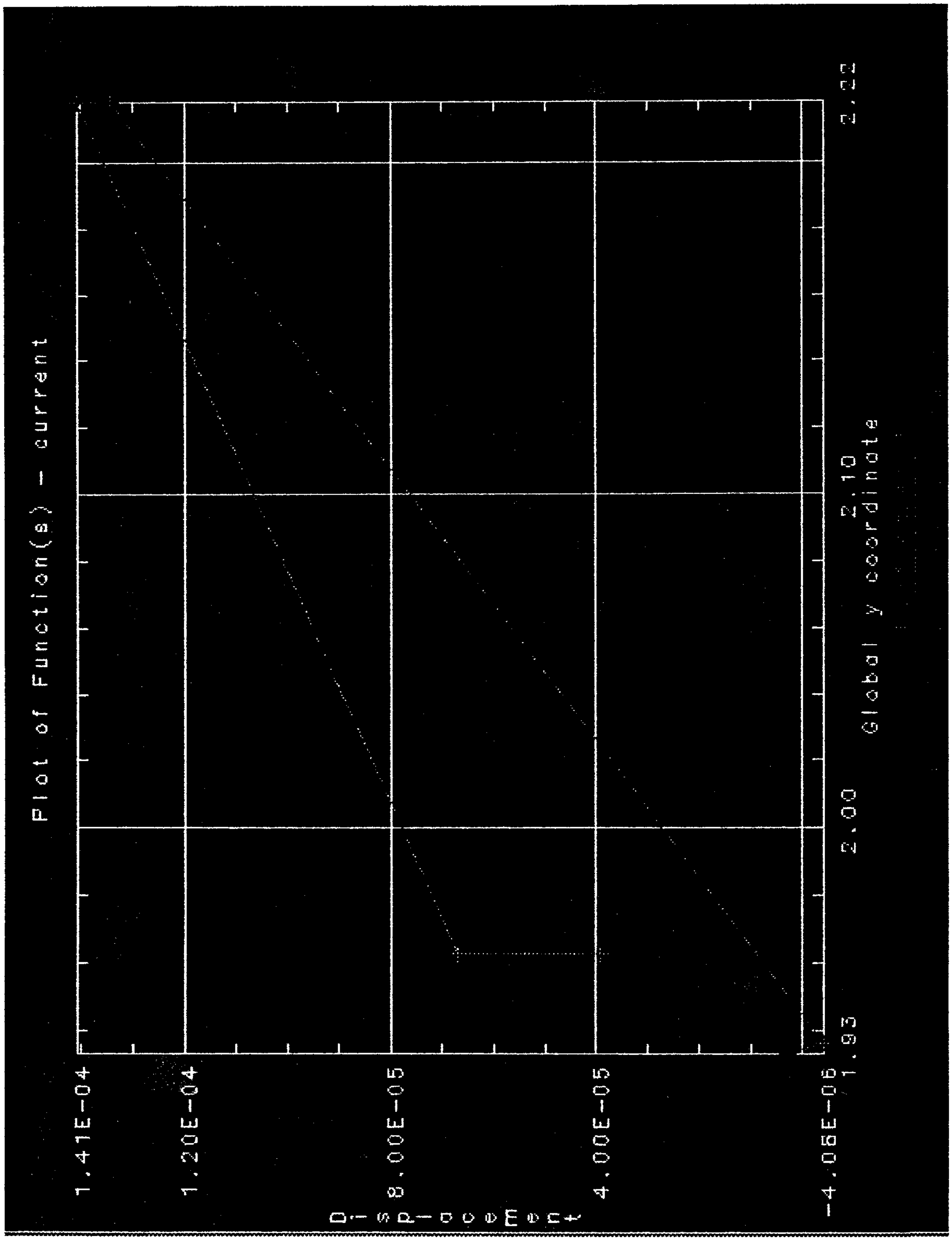

Figure 7.5 a. Displacement in Connection Area of Body and Ramus

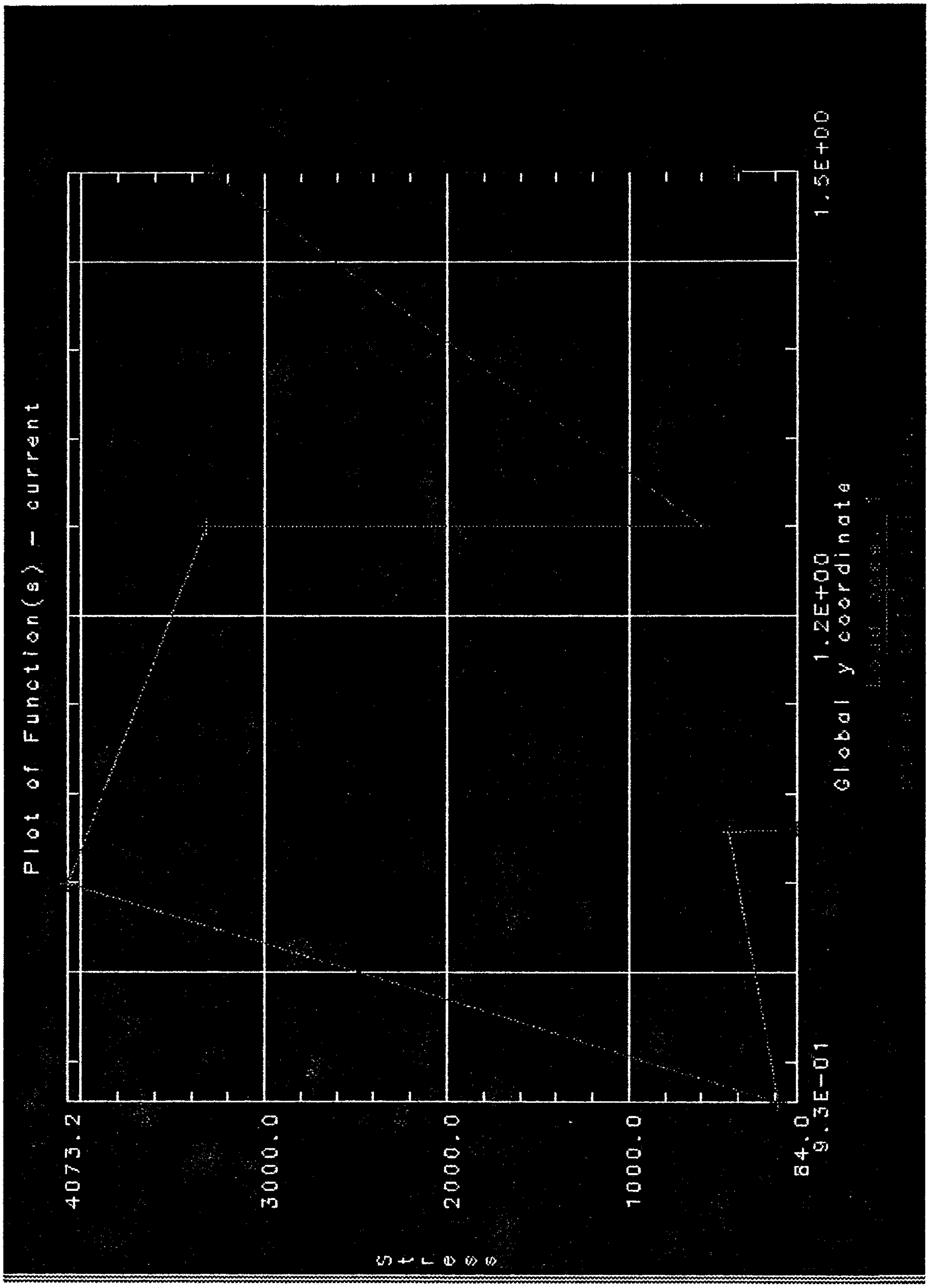

Figure 7.5 b. Maximum Principal Stress in Connection Area of Body And Ramus

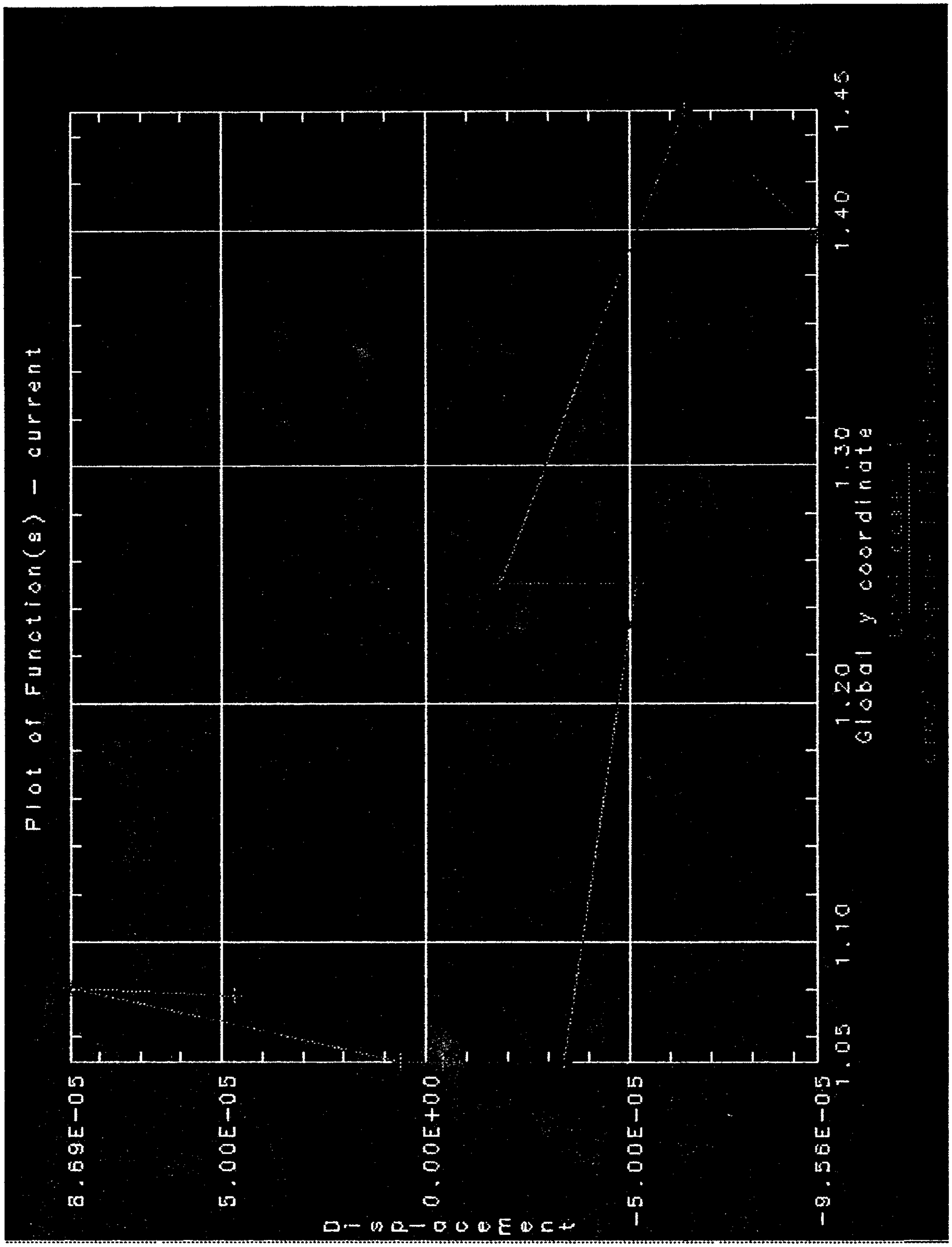

Figure 7.6 a. Displacement in Symphysis Area

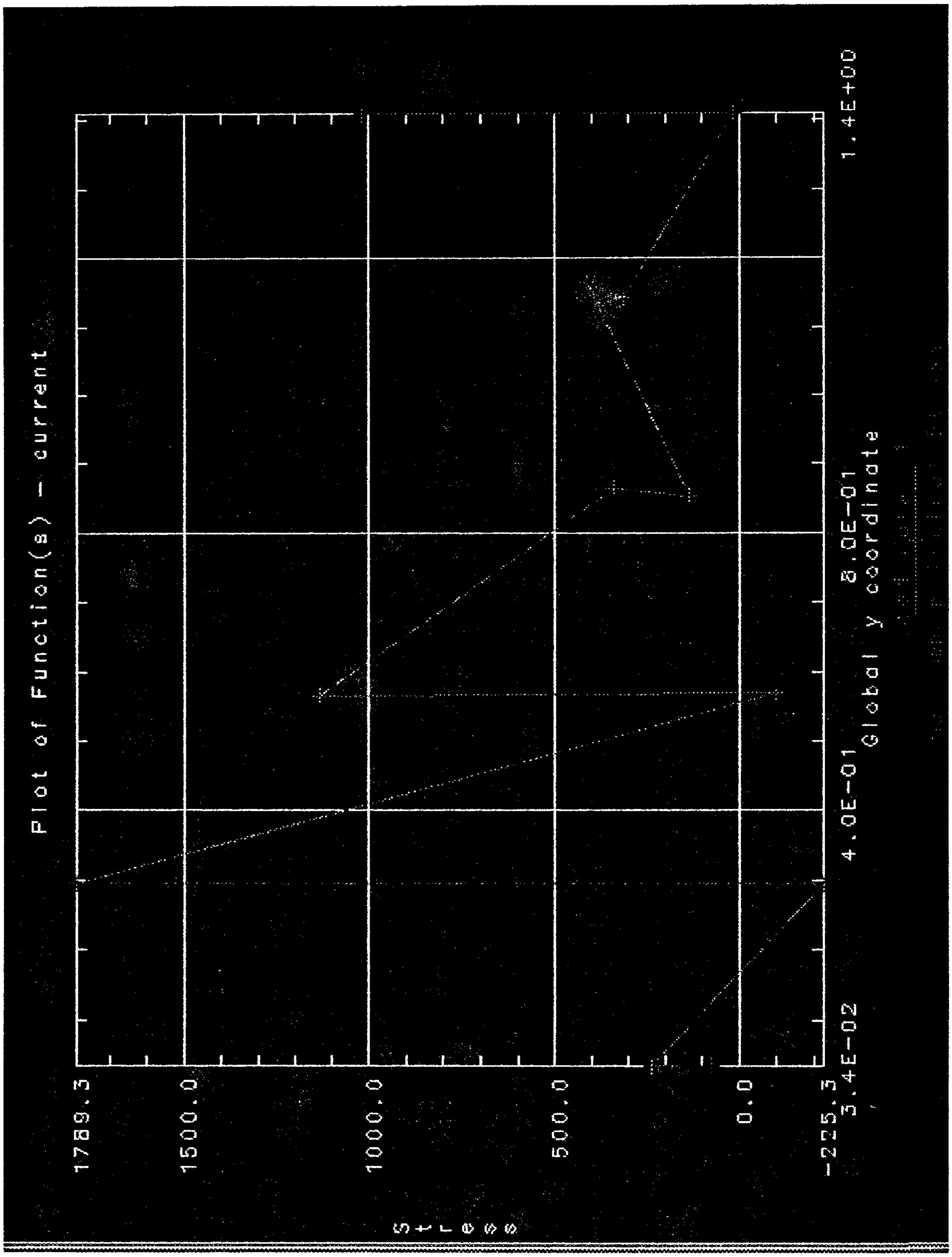

Figure 7.6 b. Maximum Principal Stress in Symphysis Area

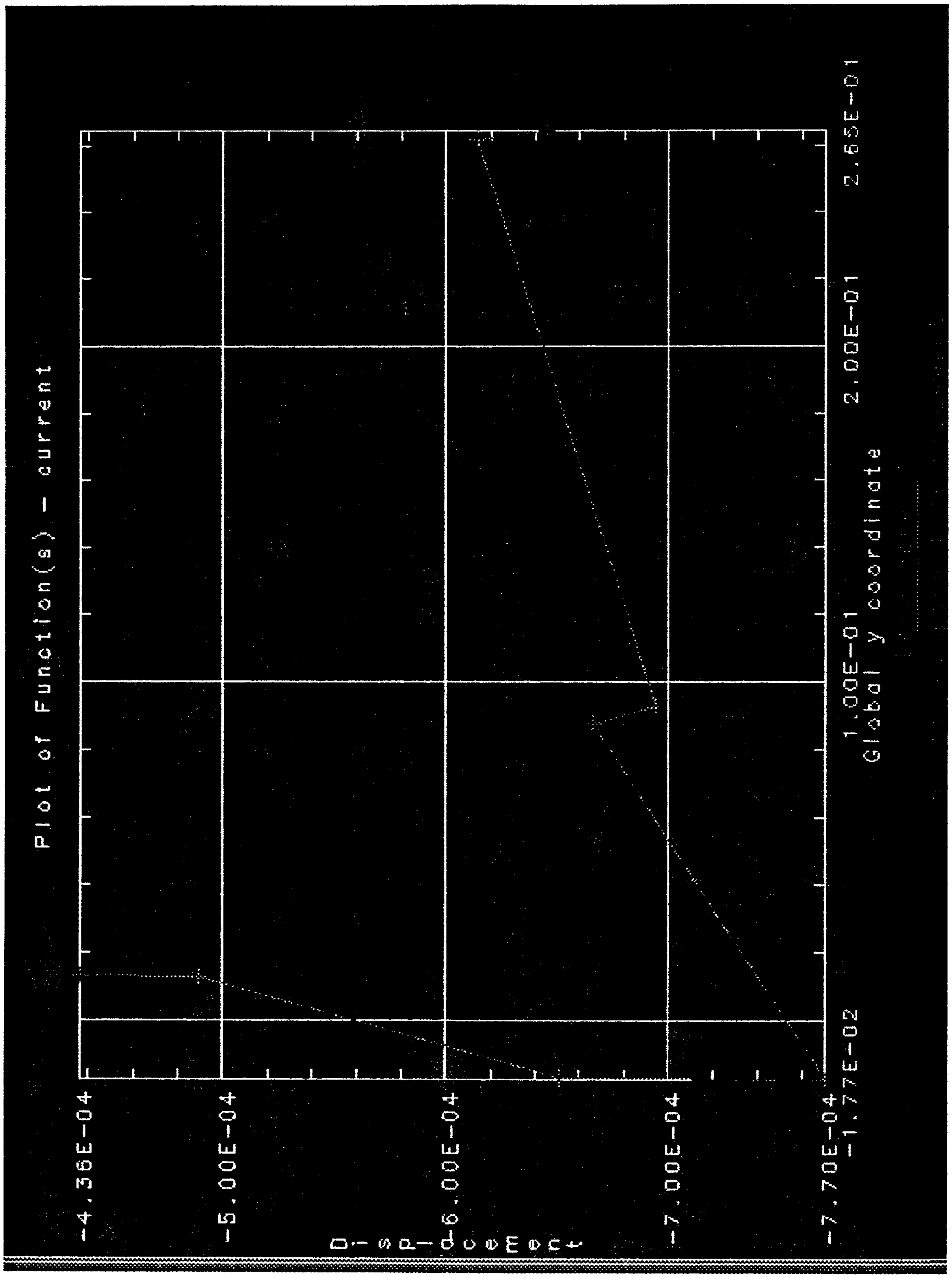

Figure 7.7 a. Displacement in Angle

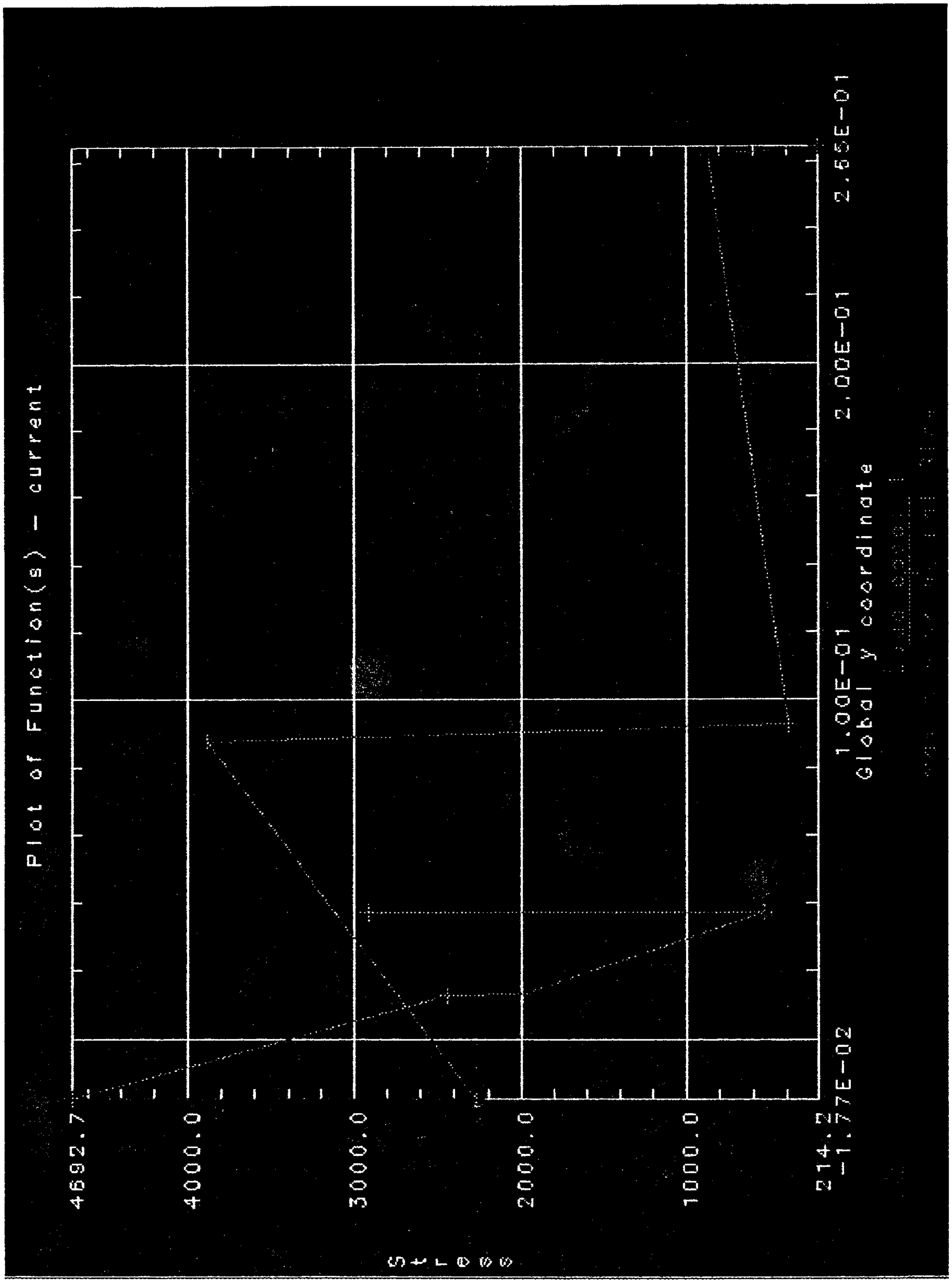

Figure 7.7 b. Maximum Principal Stress in Angle

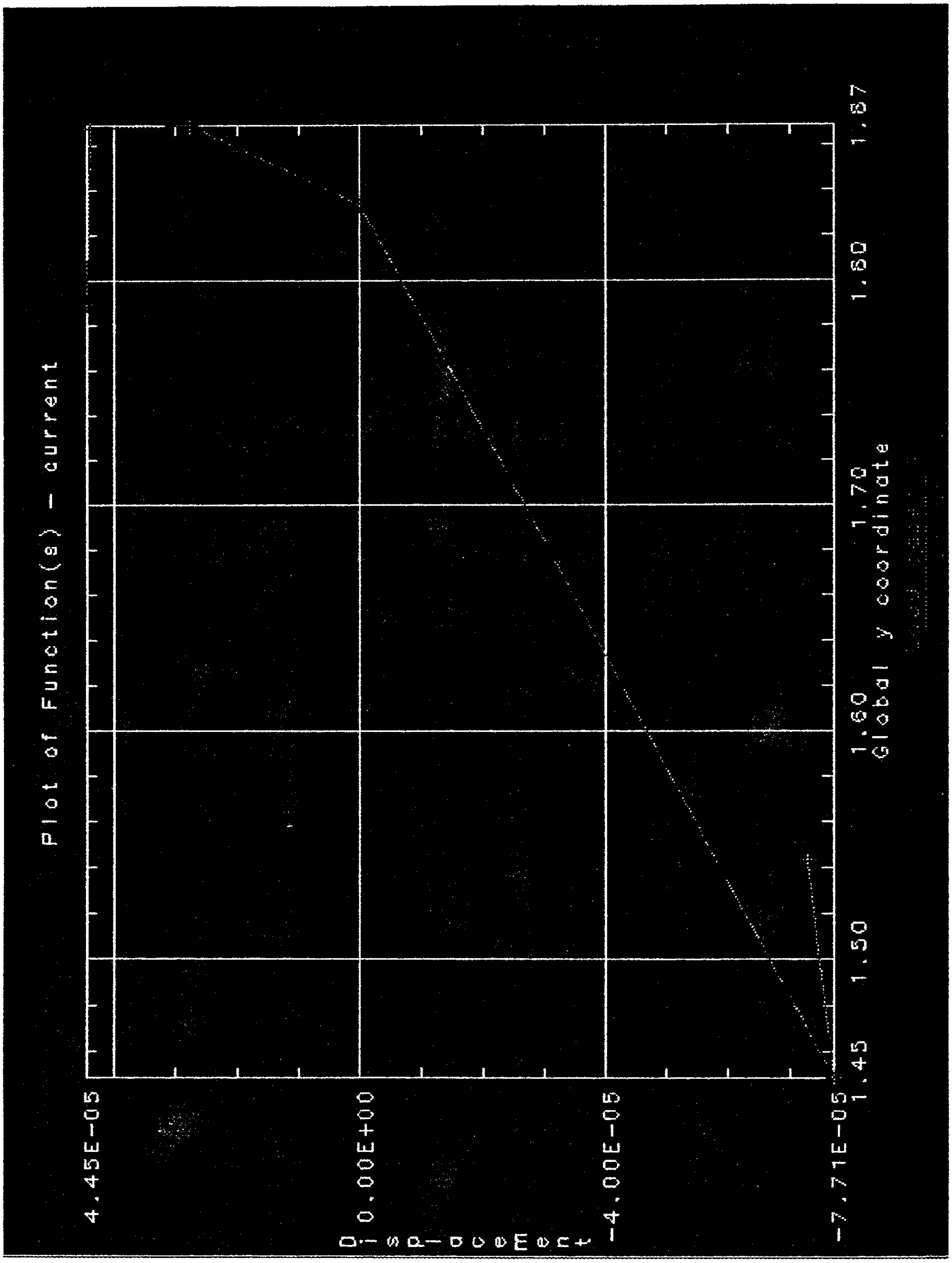

Figure 7.8 a. Displacement in Condyle Area

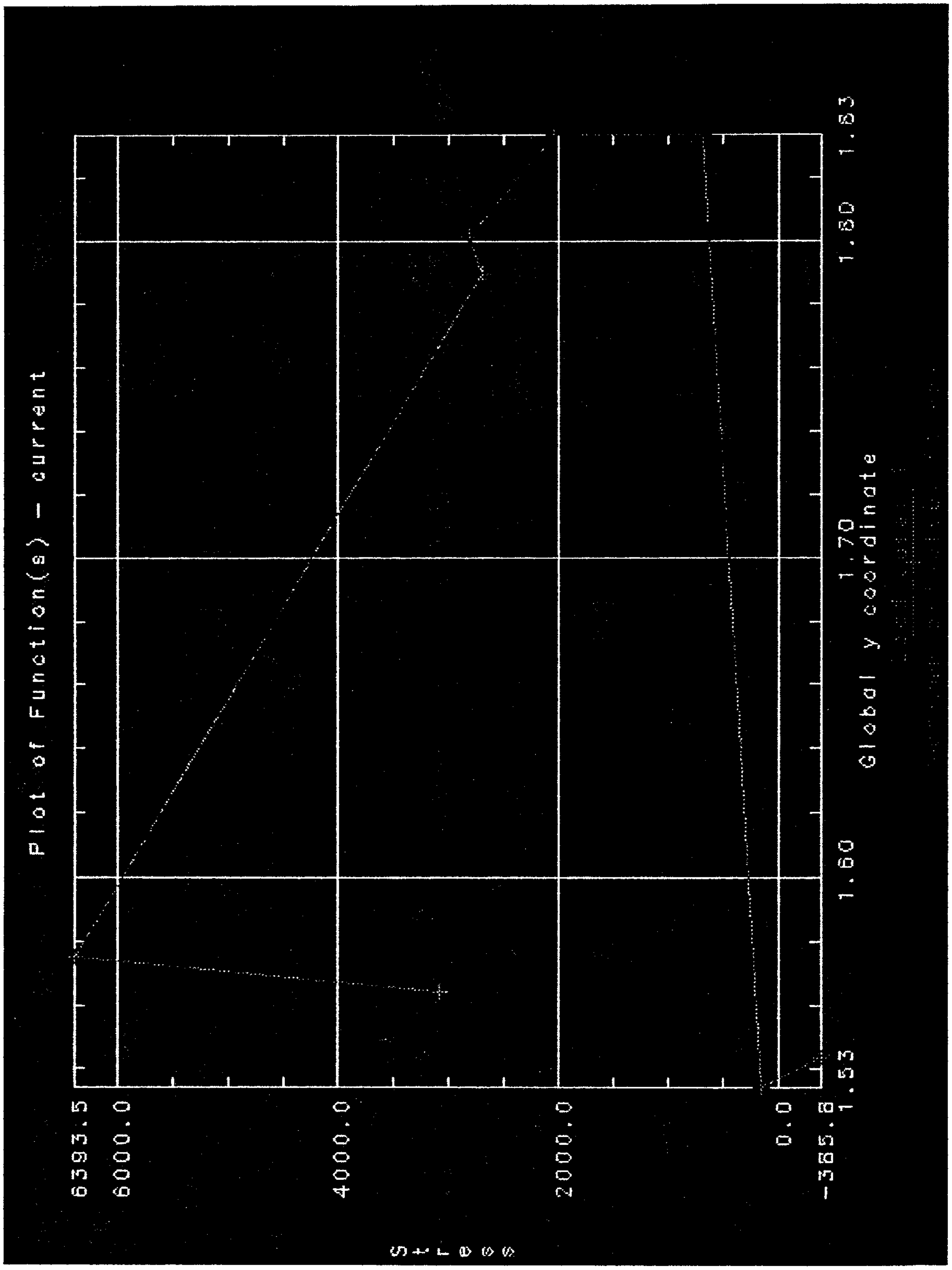

Figure 7.8 b. Maximum Principal Stress in Condyle Area

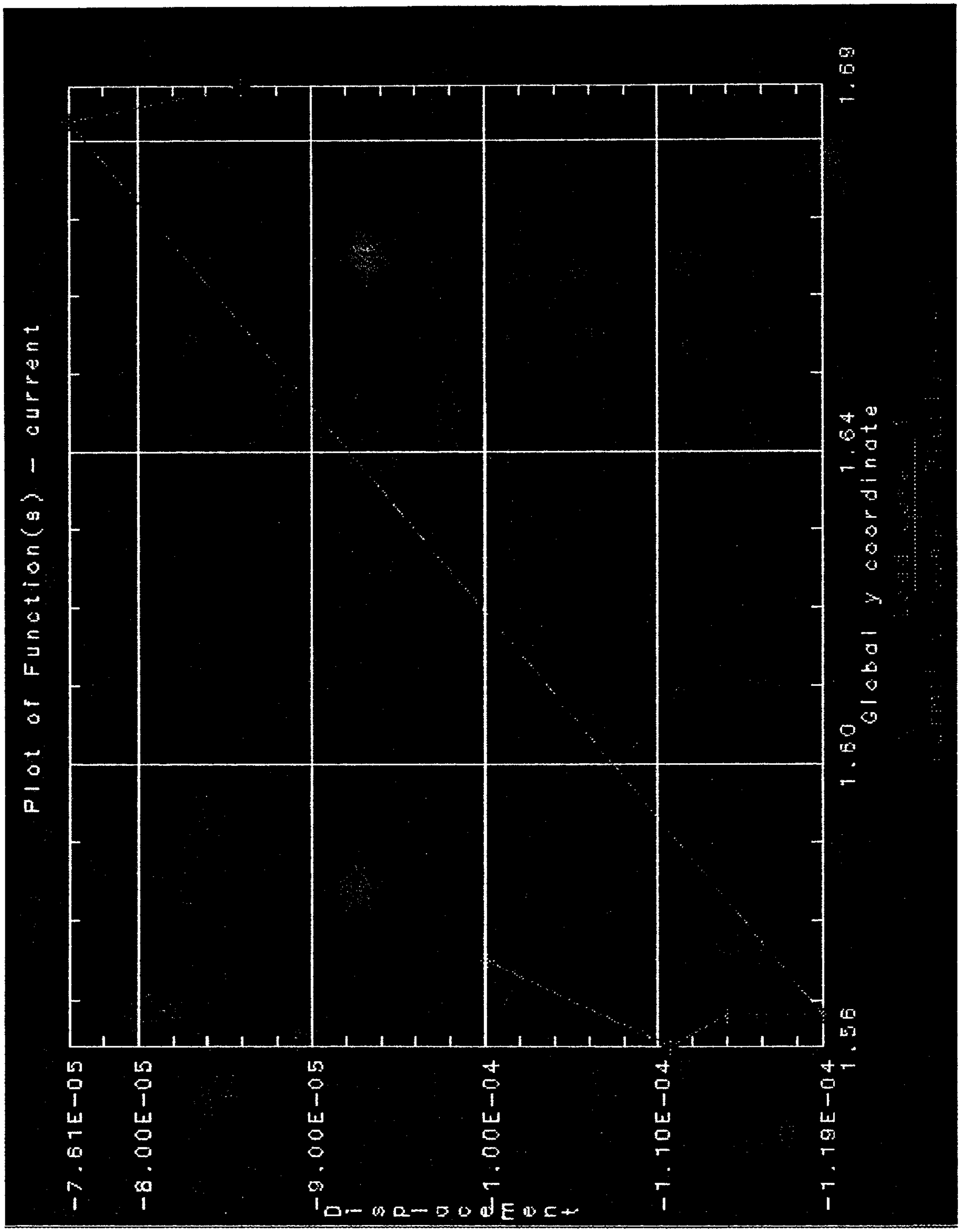

Figure 7.9 a. Displacement in Mandibular Notch Area

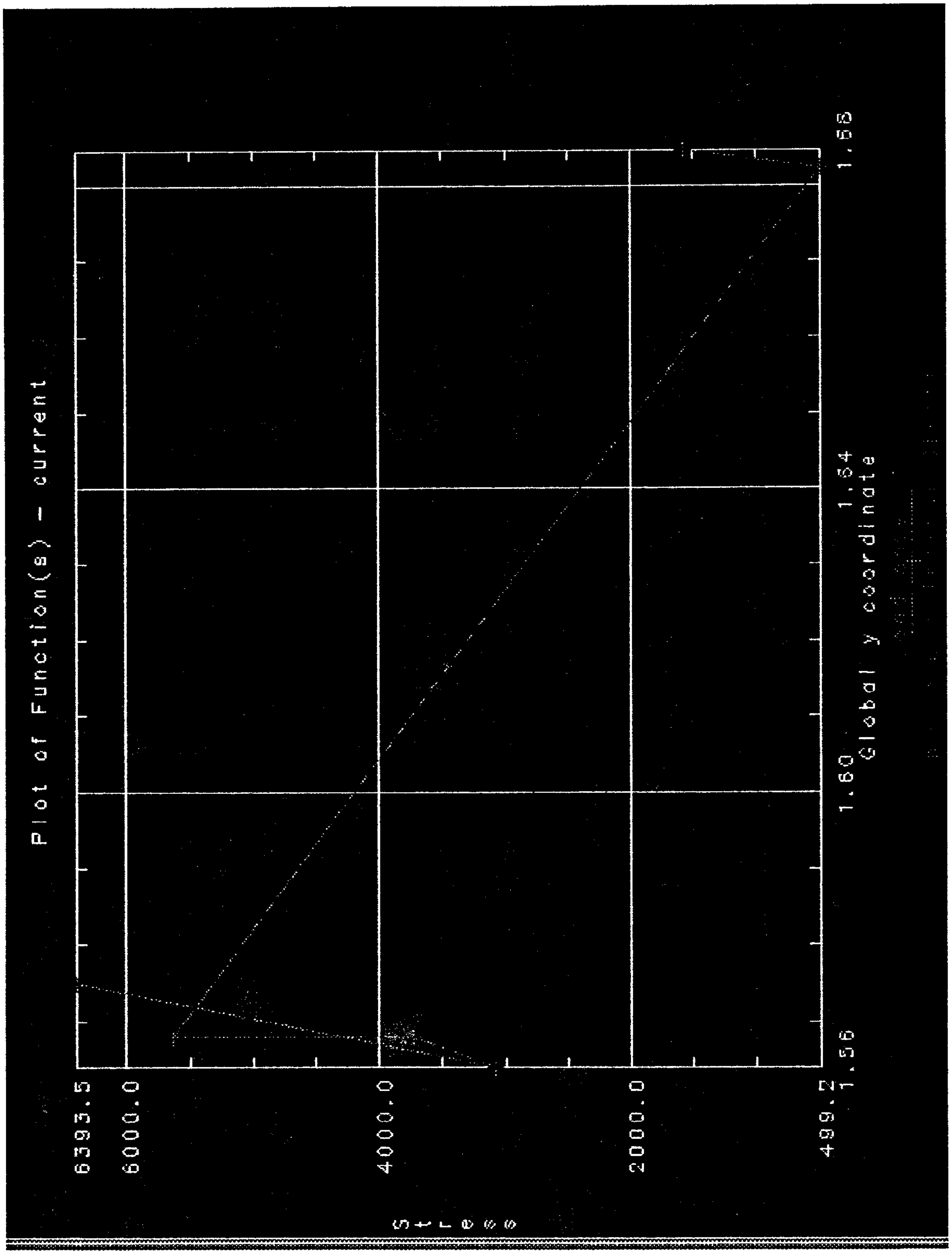

Figure 7.9 b. Maximum Principal Stress in Mandibular Notch Area

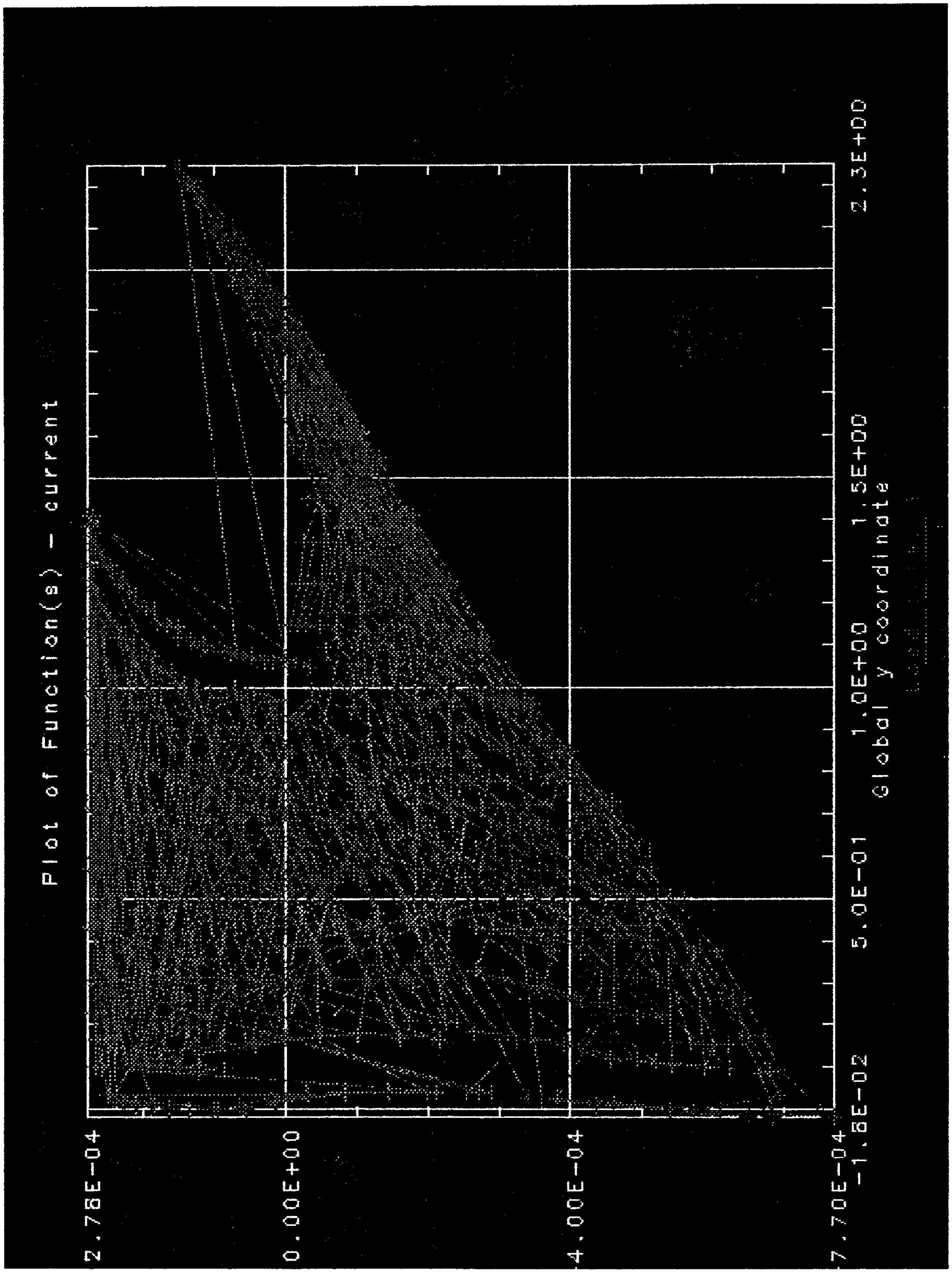

Figure 7.10 a. Whole Displacement Distribution in Mandible

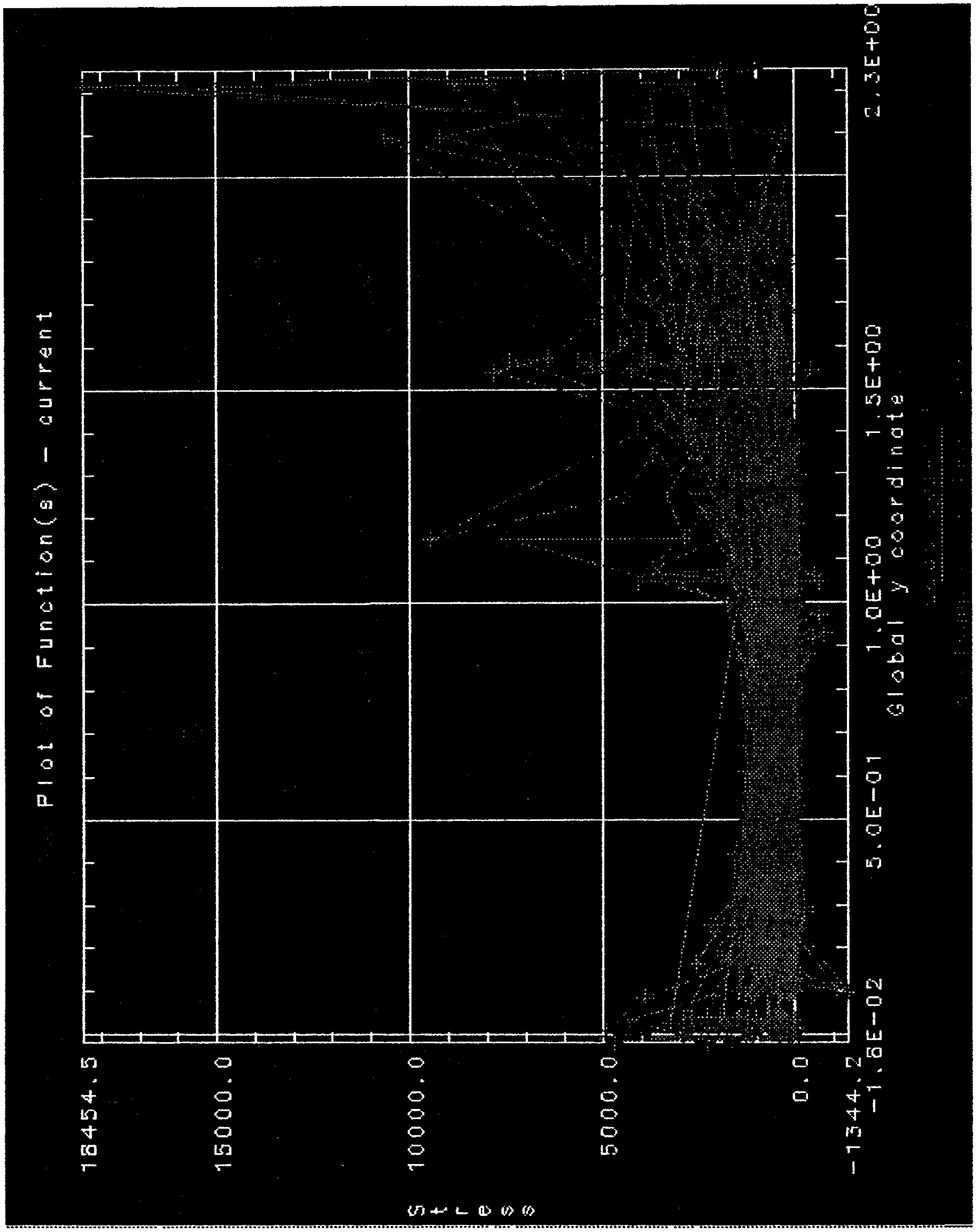

Figure 7.10 b. Whole Maximum Principal Stress Distribution in Mandible

7.2 Discussion

7.2.1 The Distribution of Displacement and Stress

From the color pictures of the distribution of displacement and stress (see Figure 7.2, 7.3), the following results were observed:

1) The maximum displacement of 8.96×10^{-2} inch occurred at the mandible angle. The second one occurred at the interior side of coronoid process and the mandible ramus. The least displacement occurred at the condyle process and middle of the mandible body; this phenomenon might be caused by the assumed constraint that condyle was a hinge and the second molar area was fixed in positive y-direction.

2) The maximum stress is about 18,400 psi and the location might be enveloped by the other elements, since it could not be seen in the picture. The higher stress is shown in the area of coronoid process; the area of notch is near the condyle process and the connection area is between the ramus and the body of the mandible. Much of the area was of low stress concentration, with the minimum stress is about -1,340 psi.

3) Compared with the cortical bone yield strength of 133 Mpa [34], i.e. 19,300 psi, the model did not indicate failure.

For a more detailed analysis, six areas were focusly studied. There were irregular distribution tendency not only in stress but in displacement (see Figure 7.4--7.9). In each plot there are dramatic changes in stress and displacement. This could be due to the fact that the stress and displacement were highly related to object geometry shape, since the areas were specified by nodes.

Because the nodes and elements were produced automatically by I-DEAS, it is difficult to specify the number of the node and element, the nodes studied were picked up by cursor on the screen. That is only the surface nodes can be picked, and the nodes were picked up arbitrarily.

Only the maximum and minimum value of stress and displacement were used as studied parameters. From Figure 7.4 a., b.--Figure 7.9 a., b. the maximum and minimum displacement and principal stress were obtained. The maximum stress and displacement and minimum stress and displacement in each plot were rearranged into the comparison table (see table 4. Table 5).

7.2.2 Data Rearrangement

Table 4: The Comparison of the Displacements (inch) in Six Selected Area

area	d_{max} (10^{-4})	d_{min} (10^{-4})	d_{max}/d_{min}	d_{max}-d_{min}
1	1.36	-0.19	-7.16	1.55
2	1.41	-0.04	-35.25	1.45
3	0.86	-0.96	-0.93	1.85
4	-4.36	-7.7	0.56	-3.34
5	0.0	-0.62	0.00	0.62
6	-0.076	-1.19	0.063	1.12

Table 5: The Comparison of the Maximum Principal Stress (psi) in Six Selected Area

area	σ_{max} (10^3)	σ_{min} (10^3)	$\sigma_{max}/\sigma_{min}$	$\sigma_{max}-\sigma_{min}$
1	8.85	0.57	15.53	8.28
2	4.07	0.084	48.49	3.96
3	1.79	-0.22	-7.95	2.01
4	4.69	0.21	21.92	4.48
5	6.39	-0.39	-16.56	6.78
6	6.39	0.50	12.80	5.89

7.2.3 Parameters for Stress Concentration

Although the plot in Figure 7.4--Figure 7.9 may difficult to understand due to irregular curve, two parameters for both displacement and stress were defined.

$$\alpha = X_{max}/X_{min} \qquad (8.1)$$

$$\beta = X_{max} - X_{min} \qquad (8.2)$$

where X is either displacement or stress.

The large value of β (both in displacement and in stress) indicates a large displacement or stress happened in that area. In other words, there are more likely a higher stress concentration appeared.

For α there are two types of situations:

1) If both the maximum and minimum value of X have the same sign, the larger α indicates a higher the stress concentration (see Table 6).

Table 6: α and β Combination Table for Stress Concentration, $\alpha > 0$

α	β	stress concentration
α >0, but large	β large	low (if absolute value is small)
α >0, but large	β large	high (if absolute value is large)
α >0, but small	β small	low (if absolute value is small)
α >0, but small	β small	high (if absolute value is large)

Table 7: α and β Combination Table for Stress Concentration, $\alpha < 0$

α	β	stress concentration
α <0, but large	β small	low
α <0, but large	β large	high
α <0, but small	β small	low
α <0, but small	β large	high

2) If both the maximum and minimum value of X have different signs, that is either X_{max} or X_{min} is under compressive stress when the other is under tensile stress. Under this circumstance, the parameter β must be considered (see Table 7).

7.2.4 Discussion

By using the Table 6 and Table 7, and considering the absolute value of stress or displacement in each area, the sequence of displacement and stress compared with other areas was obtained (see Table 8, highest 1, lowest 6).

Table 8: Relative Relation of Displacement and Maximum Principal Stress in Each Area

Area	Displacement	Stress
1.coronoid process	2	1
2.connection of body and ramus	3	2
3.symphysis	4	6
4.angle	1	5
5.condyle process	6	3
6.mandibular notch	5	4

In Table 8. it was shown that the maximum displacement occurred in the mandibular angle, then the coronoid process area, connection of body and ramus. The minimum displacement occurred in the condyle process area, since the TMJ was set up as a hinge connection as a part of boundary condition. Based on the same reason the condyle shares a third place of maximum stress. This is also due to the boundary condition that the second molar area (connection of body and ramus) is fixed in positive y-axis direction, the maximum compressive displacement occurred in the mandibular angle.

Among the selected areas, the maximum stress concentration occurred in the coronoid process. Since simulating temporalis muscle restraint force is applied and together with its thin physical shape, it is very likely of the maximum stress. Although the angle has the maximum displacement, its stress is far behind the other areas due to its thick physical shape and large area. Among those areas there is small displacement and low stress concentrated in the symphysis area, however the coronoid process area has a prominent place for both big displacement and higher stress.

7.2.5 Summary

In Figure 7.10a. (the distribution of whole mandible displacement), it is clearly shown that most of the displacements are compressive, which is caused by compressive force, the external load, applied on the symphysis. This indicates that the boundary restraint forces have minor effects on the mandible. In other words, the model successfully simulated the mastication system muscle force. The maximum displacement is 8.96×10^{-4} inch.

In Figure 7.10 b. (the distribution of whole mandible stress), the minimum stress is about -1,340 psi and the maximum stress is about 18,400 psi. The average stress is between 2,000-3,000 psi, which is far below the yield strength 19,300 psi. With the high stress concentration in a few points or area and low stress concentration in most areas, it could be concluded that in this study the model designed and the boundary condition simulation is acceptable.

It is demonstrated that along the x-axis (deep direction of mandible) there is a lower average stress distribution in the front part of the mandible. The stress goes higher from the middle part of mandible to the end of condyle, where it reaches the highest stress. There are only few points of high stress located at the end of mandible, most of those high stress areas are located on the middle part of mandible, in anatomy where the body of the mandible is.

Chapter 8
Conclusion

8.1 Conclusion

In 1985, Pantelis N. B. investigated a series of 1,521 mandibular fractures [28]. He stated that fracture of the mandibular body was the most common, and the fracture of the angle accounted for the second. Compared with the clinical investigation, our simulation indicates the similar result. Thus the simulation model and the finite element analysis are successful.

The result of this study show that the coronoid process has the maximum stress concentration. High stress concentration also occurred in the area in and near the mandibular body and mandibular angle (area 2 and area 4) where there might be the highest distributional probability of mandible fracture because of high stress concentration.

8.2 Comment

The results of this study demonstrate that I-DEAS is a suitable software package for finite element modeling and analysis. It also demonstrates that the boundary condition simulation is acceptable although a lot of detail of mastication system muscles was omitted. However, for advanced simulation of mandibular bone, more efforts should be given.

The model could be established by more accurate data such as CT-scan. The restraint force of masseter muscle could be simulated by different muscle forces such as the force of the superficial part and the deep part of masseter muscle, and the pterygoid muscles. Also the model could be considered with different material properties, such as inhomogenious, that is the composition structure of cortical bone combined with the cancellous bone.

Appendix

Appendix 1 Mandible Measured Data

Table 9: Data of Mandible (inch) Measured by Optical Comparator

number	x	y	z
1	0.000	0.294	0.000
2	0.000	0.294	-0.367
3	-0.219	0.052	-0.002
4	-0.219	0.052	-0.387
5	-0.219	0.826	-0.002
6	-0.219	0.826	-0.200
7	-0.328	0.034	-0.002
8	-0.328	0.034	-0.389
9	-0.328	1.133	-0.002
10	-0.328	1.133	-0.200
11	-0.328	1.411	-0.003
12	-0.328	1.411	-0.424
13	-0.743	0.000	-0.607
14	-0.743	0.000	-1.107
15	-0.743	1.292	-0.424
16	-0.743	1.292	-0.661
17	-0.979	0.000	-0.850
18	-0.979	0.000	-1.270
19	-0.979	1.198	-0.606
20	-0.979	1.198	-1.196
21	-1.316	0.038	-1.044
22	-1.316	0.038	-1.464

Table 9: Data of Mandible (inch) Measured by Optical Comparator

number	x	y	z
23	-1.316	1.105	-0.709
24	-1.316	1.105	-1.129
25	-1.683	0.042	-1.172
26	-1.683	0.042	-1.551
27	-1.683	1.068	-0.840
28	-1.683	1.068	-1.392
29	-1.834	0.038	-1.361
30	-1.834	0.038	-1.611
31	-1.834	1.049	-0.876
32	-1.834	1.049	-1.496
33	-2.243	0.000	-1.529
34	-2.243	0.000	-1.744
35	-2.243	1.451	-1.120
36	-2.243	1.451	-1.540
37	-2.535	0.000	-1.576
38	-2.535	0.000	-1.766
39	-2.535	2.218	-1.335
40	-2.535	2.218	-1.642
41	-2.672	0.081	-1.606
42	-2.672	0.081	-1.784
43	-2.672	2.250	-1.398
44	-2.672	2.250	-1.576
45	-2.872	0.212	-1.630
46	-2.872	0.212	-1.822
47	-2.872	1.730	-1.494
48	-2.872	1.730	-1.657
49	-3.119	0.504	-1.621

Table 9: Data of Mandible (inch) Measured by Optical Comparator

number	x	y	z
50	-3.119	0.504	-1.871
51	-3.119	1.568	-1.627
52	-3.119	1.568	-1.763
53	-3.459	0.958	-1.704
54	-3.459	0.958	-1.852
55	-3.459	1.603	-1.704
56	-3.459	1.603	-1.952
57	-3.719	1.226	-1.600
58	-3.719	1.226	-1.999
59	-3.719	1.868	-1.683
60	-3.719	1.868	-2.026
61	-3.855	1.360	-1.600
62	-3.855	1.360	-2.067
63	-3.855	1.834	-1.614
64	-3.855	1.834	-1.614

Here, according to the coordinate definition of I-DEAS, the x-axis is the depth in the sagittal plane, the y-axis is the height in the sagittal plane and z-axis is the width in the transverse plane. see Figure A1.1

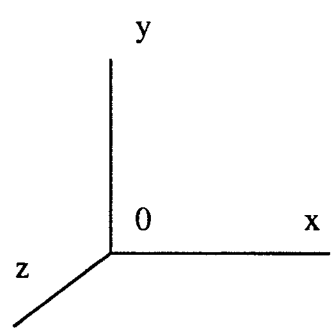

Figure A1.1 The Coordinate Definition of I-DEAS

Appendix 2 The Program for Mandible Model Establishment

```
K : /
K : CR
K : SP
K : K
K : -0.328,1.410,-0.003
K : -0.328,1.133,-0.002
K : -0.219,0.826,-0.002
K :  0.000,0.294, 0.000
K : d
K :
K :  0.000,0.294, 0.000
K : -0.219,0.052,-0.002
K : -0.328,0.034,-0.002
K : d
K :
K : -0.743,0.000,-0.607
K : -0.979,0.000,-0.850
K : -1.316,0.038,-1.044
K : -1.683,0.042,-1.172
K : -1.834,0.038,-1.361
K : d
K : d
K : l
K : si
K : K
K : -1.834,0.038,-1.361
K : -1.834,1.049,-0.876
K : d
K : /m
K : cr
K : sp
K : K
K : -1.834,1.049,-0.876
K : -1.683,1.068,-0.840
K : -1.316,1.105,-0.709
K : -0.979,1.198,-0.606
K : -0.743,1.292,-0.424
K : -0.328,1.411,-0.003
K : d
K : d
K :
K : l
K : si
K : K
K : -0.328,1.411,-0.003
K : -0.328,1.411,-0.424
K : -0.328,0.034,-0.002
K : -0.328,0.034,-0.389
K : -1.834,0.038,-1.361
K : -1.834,0.038,-1.611
K : -1.834,1.049,-0.876
K : -1.834,1.049,-1.496
K : d
K : /m
K : V
K : E
K : 3 4 5
K :
K : AU
K : /
K : CR
K : SP
K : K
K : -1.834,1.049,-1.496
K : -1.683,1.068,-1.392
K : -1.316,1.105,-1.129
K : -0.979,1.198,-1.006
K : -0.743,1.292,-0.661
K : -0.328,1.411,-0.424
K : d
K : -0.328,1.411,-0.424
K : -0.328,1.133,-0.002
K : !
K : -0.328,1.133,-0.200
K : -0.219,0.826,-0.200
K :  0.000,0.295,-0.367
```

```
K : d
K : K
K : 0.000, 0.294,-0.367
K : -0.219,0.052,-0.387
K : -0.328,0.034,-0.389
K : d
K :
K : -0.743,0.000,-1.107
K : -0.979,0.000,-1.270
K : -1.316,0.037,-1.464
K : -1.683,0.042,-1.551
K : -1.834,0.037,-1.611
K : d
K : d
K : l
K : si
K : K
K : -1.834,0.037,-1.611
K : -1.834,1.049,-1.496
K : D
K : /
K : V
K : E
K : 3 4 5
K : /
K : CR
K : SP
K : K
K : -1.834,0.037,-1.361
K : -2.243,0.000,-1.529
K : -2.535,0.000,-1.576
K : -2.672,0.081,-1.606
K : -2.872,0.212,-1.630
K : -3.119,0.504,-1.621
K : D
K : D
K : AU
K : L
K : SI
K : K
K : -3.119,0.504,-1.621
K : -1.834,1.049,-0.876
K :
K : -1.834,1.049,-1.496
K :
K : -3.119,0.504,-1.871
K :
K : -3.119,0.504,-1.621
K : !
K : d
K : AU
K : SI
K : K
K : -3.119,0.504,-1.621
K : -3.119,0.504,-1.871
K : D
K : /
K : CR
K : SP
K : K
K : -3.119,0.504,-1.871
K : -2.872,0.212,-1.822
K : -2.672,0.081,-1.784
K : -2.535,0.000,-1.766
K : !
K : -2.535,0.000,-1.766
K : -2.243,0.000,-1.744
K : -1.834,0.038,-1.611
K : D
K : D
K : AU
K : L
K : SI
K : K
K : -1.834,1.049,-0.876
K : -2.243,1.451,-1.120
K :
K : -3.459,0.958,-1.704
K :
K : -3.119,0.504,-1.621
```

```
K : -3.119,0.504,-1.871
K : -3.459,0.958,-1.852
K : !
K : !
K : -3.459,0.958,-1.852
K :
K : -2.243,1.451,-1.540
K :
K : -1.834,1.049,-1.496
K : D
K : AU
K : SI
K : K
K : -3.459,0.958,-1.704
K : -3.119,1.568,-1.627
K :
K : -2.243,1.451,-1.120
K :
K : -2.243,1.451,-1.540
K :
K : -3.119,1.568,-1.763
K :
K : -3.459,0.958,-1.852
K :
K : -3.459,0.958,-1.704
K : D
K : AU
K : SI
K : K
K : -2.243,1.451,-1.120
K : -2.535,2.218,-1.335
K :
K : -2.535,2.218,-1.642
K :
K : -2.243,1.451,-1.540
K : D
K : SI
K : K
K :
K : !
K : D
K : AU
K : /
K : CR
K : SP
K : K
K : -2.535,2.218,-1.335
K : -2.672,2.250,-1.398
K : -2.872,1.730,-1.494
K : -3.119,1.568,-1.627
K : D
K : -3.119,1.568,-1.763
K : -2.872,1.730,-1.657
K : -2.672,2.250,-1.576
K : -2.535,2.218,-1.642
K : D
K : -3.119,1.568,-1.763
K : !
K : -3.119,2.218,-1.627
K : !
K : -3.119,1.568,-1.627
K : -3.459,1.603,-1.952
K : -3.719,1.868,-2.026
K : !
K : !
K : -3.459,1.603,-1.704
K : -3.719,1.868,-1.685
K : -3.855,1.834,-1.614
K : D
K : K
K : -3.855,1.834,-1.614
K : -3.855,1.360,-1.600
K : -3.719,1.226,-1.600
K : -3.459,0.958,-1.704
K : D
K : K
K : -3.459,0.958,-1.852
K : -3.719,1.226,-1.999
K : -3.855,1.360,-2.067
K : -3.855,1.834,-2.087
```

```
K : D
K : K
K : -3.855,1.834,-2.087
K : -3.719,1.868,-2.026
K : -3.459,1.603,-1.952
K : -3.119,1.568,-1.763
K : d
K : D
K : L
K : SI
K : K
K : -3.119,1.568,-1.627
K : -3.119,1.568,-1.763
K : D
K : l
K : si
K : K
K : -3.855,1.834,-1.614
K : -3.855,1.834,-2.087
K : d
K : l
K : si
K : K
K : -3.119,0.504,-1.871
K : -3.459,0.958,-1.852
K : d
K : l
K : si
K : K
K : 0.000,0.294, 0.000
K : 0.000,0.294,-0.367
K : d
K : AU
K : /
K : MF
K : PR
K : E
E : **** END OF SESSION ****
```

The meanings of the major language is explained in following examples, for more detail of I-DEAS program language, I-DEAS MENU GUIDE should be checked.

examples:

```
D: done
K: keyin data
L: line
SI: single line
SP: spline
CR: create
MF: model file
PR: program
E: end
```

Appendix 3

Basic Principle of Three Dimension Finite Element Analysis

A3.1 Basic Stress-Strain Relation

If the displacement is :

$$u = [u, v, w]^T \tag{A3.1}$$

where u, v, and w are displacements in the x, y, and z directions, respectively. The stresses and strains[17] are given by

$$\sigma = [\sigma_x, \sigma_y, \sigma_z, \tau_{yz}, \tau_{xz}, \tau_{xy}]^T \tag{A3.2}$$

$$\varepsilon = [\varepsilon_x, \varepsilon_y, \varepsilon_z, \gamma_{yz}, \gamma_{xz}, \gamma_{xy}]^T \tag{A3.3}$$

The stress-strain relations are given by

$$\sigma = \varepsilon D \tag{A3.4}$$

For isotropic materials

$$D = \frac{E}{2(1+\nu)(1-2\nu)} \begin{bmatrix} 2-2\nu & \nu & \nu & 0 & 0 & 0 \\ \nu & 2-2\nu & \nu & 0 & 0 & 0 \\ \nu & \nu & 2-2\nu & 0 & 0 & 0 \\ 0 & 0 & 0 & 1-2\nu & 0 & 0 \\ 0 & 0 & 0 & 0 & 1-2\nu & 0 \\ 0 & 0 & 0 & 0 & 0 & 1-2\nu \end{bmatrix} \tag{A3.5}$$

$$\varepsilon = \left[\frac{\partial u}{\partial x}, \frac{\partial v}{\partial y}, \frac{\partial w}{\partial z}, \left(\frac{\partial w}{\partial y} + \frac{\partial v}{\partial z}\right), \left(\frac{\partial w}{\partial x} + \frac{\partial u}{\partial z}\right), \left(\frac{\partial u}{\partial y} + \frac{\partial v}{\partial x}\right)\right] \tag{A3.6}$$

A3.2 Tetrahedra Mesh and Finite Element Formulation

Although there are several kinds of meshes in three dimension finite elment, it will only focus on the tetrahedra element in this study. A typical element is show in Figure A3.1. If for each node , the degree of freedom is three, then the local and global displacement vectors are:

$$q = [q_1, q_2, q_3, q_4, q_5, q_6, q_7, q_8, q_9, q_{10}, q_{11}, q_{12}]^T$$
$$Q = [Q_1, Q_2, Q_3, Q_4, Q_5, Q_6, Q_7, Q_8, Q_9, Q_{10}, Q_{11}, Q_{12}]^T$$

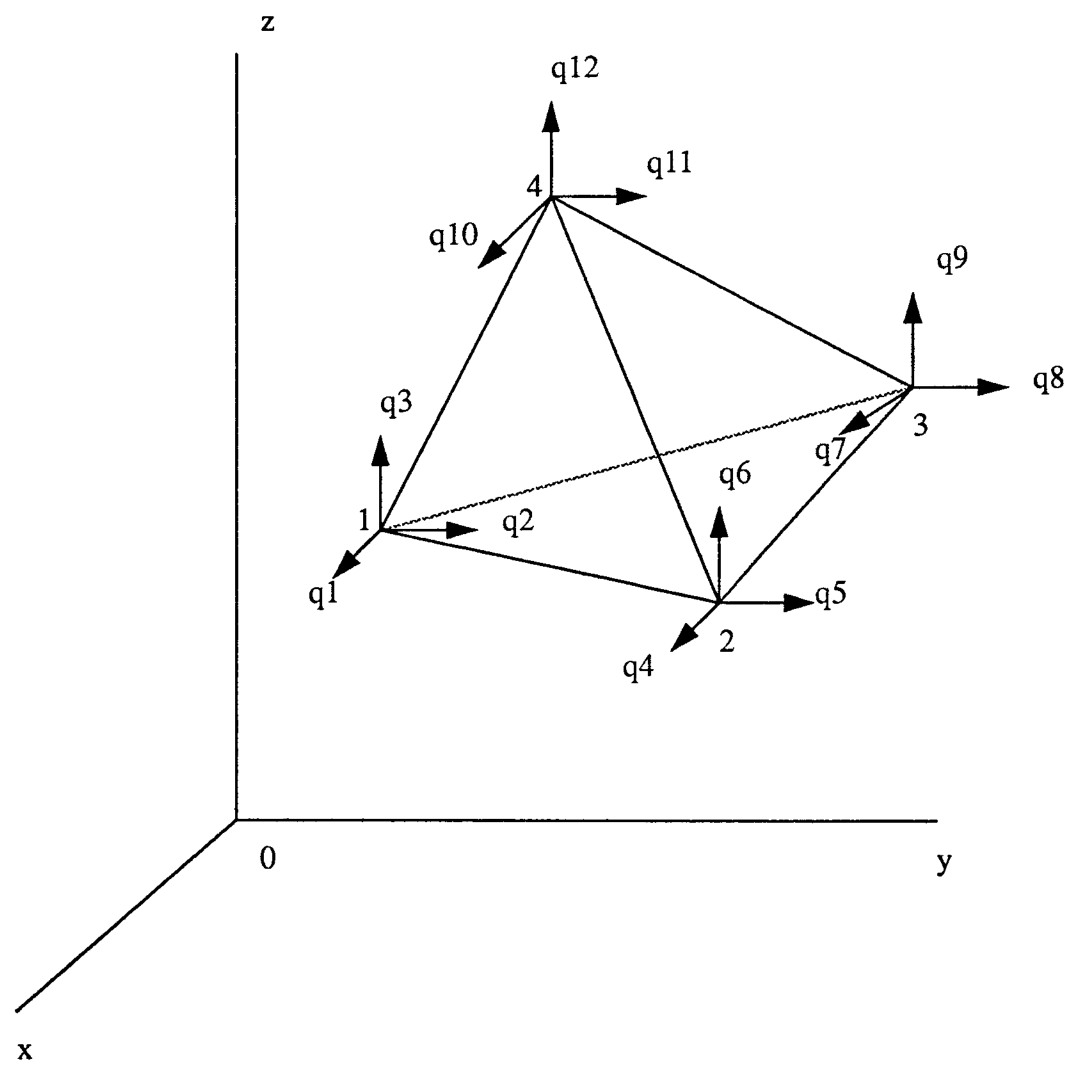

Figure A3.1 Tetrahedral Element

then the Lagrange-type shape functions are:

$$N_1 = \xi \tag{A3.7}$$

$$N_2 = \eta \tag{A3.8}$$

$$N_3 = \zeta \tag{A3.9}$$

$$N_4 = 1 - \xi - \eta - \zeta \tag{A3.10}$$

where shape function Ni has a value of 1 at node i and is zero at the other three nodes, as shown in Figure A3.2.

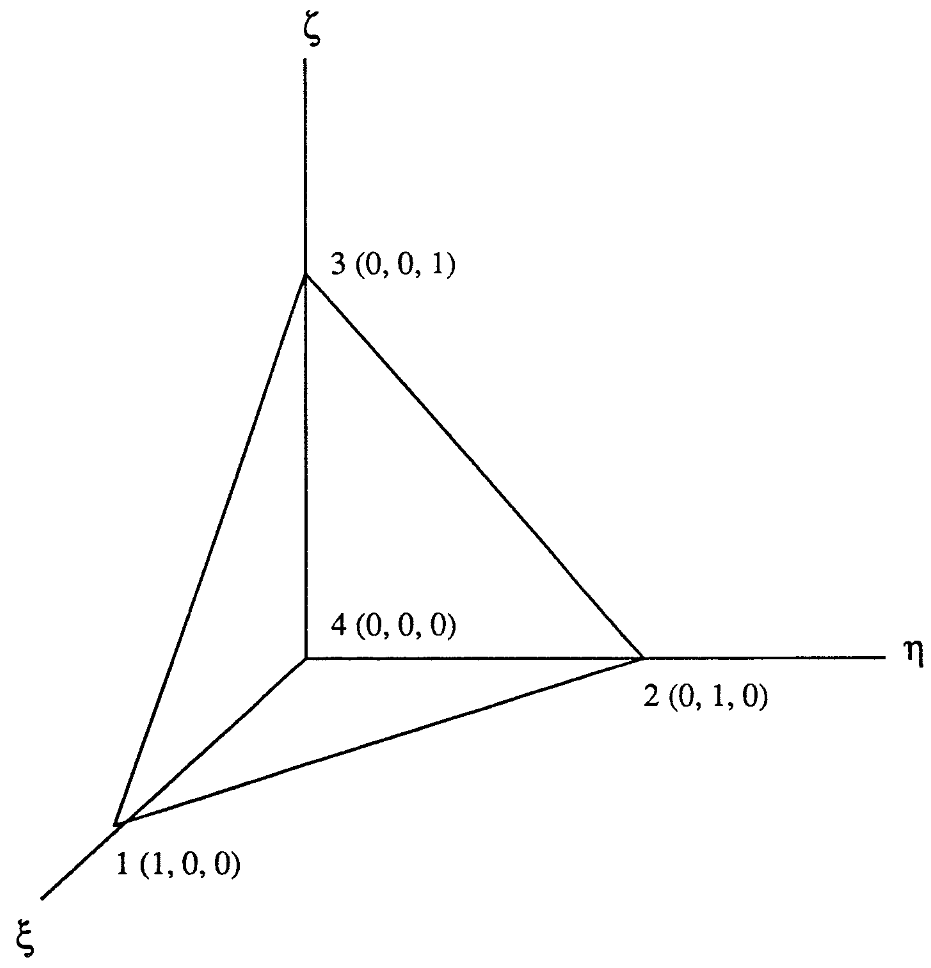

Figure A3.2 Master Element for Shape Functions

The displacements u, v, w can be written in terms of the unknown nodal values as

$$u = Nq \tag{A3.11}$$

$$N = \begin{bmatrix} N_1 & 0 & 0 & N_2 & 0 & 0 & N_3 & 0 & 0 & N_4 & 0 & 0 \\ 0 & N_1 & 0 & 0 & N_2 & 0 & 0 & N_3 & 0 & 0 & N_4 & 0 \\ 0 & 0 & N_1 & 0 & 0 & N_2 & 0 & 0 & N_3 & 0 & 0 & N_4 \end{bmatrix} \tag{A3.12}$$

The isoparametric transformation can be given by

$$x = N_1 x_1 + N_2 x_2 + N_3 x_3 + N_4 x_4 \tag{A3.13}$$

$$y = N_1 y_1 + N_2 y_2 + N_3 y_3 + N_4 y_4 \tag{A3.14}$$

$$z = N_1 z_1 + N_2 z_2 + N_3 z_3 + N_4 z_4 \tag{A3.15}$$

substituting the shape functions and using the notation $x_{ij} = x_i - x_j$,$y_{ij} = y_i - y_j$ and $z_{ij} = z_i - z_j$, yields

$$x = x_4 + x_{14}\xi + x_{24}\eta + x_{34}\zeta \tag{A3.16}$$

$$y = y_4 + y_{14}\xi + y_{24}\eta + y_{34}\zeta \tag{A3.17}$$

$$z = z_4 + z_{14}\xi + z_{24}\eta + z_{34}\zeta \tag{A3.18}$$

therefore , for u

$$\begin{bmatrix} \frac{\partial u}{\partial \xi} \\ \frac{\partial u}{\partial \eta} \\ \frac{\partial u}{\partial \zeta} \end{bmatrix} = J \begin{bmatrix} \frac{\partial u}{\partial x} \\ \frac{\partial u}{\partial y} \\ \frac{\partial u}{\partial z} \end{bmatrix} \tag{A3.19}$$

The Jacobean transformation is given by

$$J = \begin{bmatrix} \frac{\partial x}{\partial \xi} & \frac{\partial y}{\partial \xi} & \frac{\partial z}{\partial \xi} \\ \frac{\partial x}{\partial \eta} & \frac{\partial y}{\partial \eta} & \frac{\partial z}{\partial \eta} \\ \frac{\partial x}{\partial \zeta} & \frac{\partial y}{\partial \zeta} & \frac{\partial z}{\partial \zeta} \end{bmatrix} = \begin{bmatrix} x_{14} & y_{14} & z_{14} \\ x_{24} & y_{24} & z_{24} \\ x_{34} & y_{34} & z_{34} \end{bmatrix} \tag{A3.20}$$

The inverse relation corresponding to equation (A3.19) is given by

$$\begin{bmatrix} \frac{\partial u}{\partial x} \\ \frac{\partial u}{\partial y} \\ \frac{\partial u}{\partial z} \end{bmatrix} = A \begin{bmatrix} \frac{\partial u}{\partial \xi} \\ \frac{\partial u}{\partial \eta} \\ \frac{\partial u}{\partial \zeta} \end{bmatrix}$$

where A is the inverse of the Jacobean matrix J, combining with equations (A3.6) and (A3.11), get:

$$\varepsilon = Bq \tag{A3.22}$$

where $B = NA$

A3.3 Element Stiffness

The element strain energy in the total potential is given by

$$U_e = \frac{1}{2}\int_e \varepsilon^T D \varepsilon dV \tag{A3.23}$$

combining with equation (A3.22), we get

$$U_e = \frac{1}{2} q^T k^e q \tag{A3.24}$$

where k^e is the element stiffness matrix, given by:

$$k^e = V_e B^T D B \tag{A3.25}$$

A3.4 Stress Calculations

Combining equations (A3.4) and (A3.22) together, we will get the element stress

$$\sigma = DBq \tag{A3.26}$$

The three principal stresses can be calculated by using the following relationships.

The three invariants of the stress tensor are:

$$I_1 = \sigma_x + \sigma_y + \sigma_z \tag{A3.27}$$

$$I_2 = \sigma_x\sigma_y + \sigma_y\sigma_z + \sigma_z\sigma_x - \tau_{yz}^2 - \tau_{xz}^2 - \tau_{xy}^2 \tag{A3.28}$$

$$I_3 = \sigma_x\sigma_y\sigma_z + 2\tau_{yz}\tau_{xz}\tau_{xy} - \sigma_x\tau_{yz}^2 - \sigma_y\tau_{xz}^2 - \sigma_z\tau_{xy}^2 \tag{A3.29}$$

The principal stresses are given by:

$$\sigma_1 = I_1/3 + c\cos\theta \tag{A3.30}$$

$$\sigma_2 = I_1/3 + c\cos\left(\theta + (2\pi)/3\right) \tag{A3.31}$$

$$\sigma_3 = I_1/3 + c\cos\left(\theta + (4\pi)/3\right) \tag{A.32}$$

where :

$$a = I_1^2/3 - I_2 \tag{A3.33}$$

$$b = -2\left(I_1/3\right)^3 + \left(I_1I_2\right)/3 - I_3 \tag{A3.34}$$

$$c = 2\sqrt{\frac{a}{3}} \tag{A3.35}$$

$$\theta = \frac{1}{3}\operatorname{acos}\left(-3\frac{b}{ac}\right) \tag{A3.36}$$

Appendix 4 Simply Test of I-DEAS Accuracy

A4.1Flexure Formula

The normal stress at any distance y from the neutral surface can be calculated by flexure formula [33]

$$\sigma = (-M)\frac{y}{I} \tag{A4.1}$$

where, M is the resisting moment at the cross section where the normal stress is to be calculated, I is the moment of inertia of the cross section relative to its neutral axis and y is the distance of a point in the cross section from the neutral axis.

For a 10 inch long rectangular cantilever beam with 1 inch wide and 2 inch heigh. when structural load 100lb is applied at the free end.see Figure A4.1

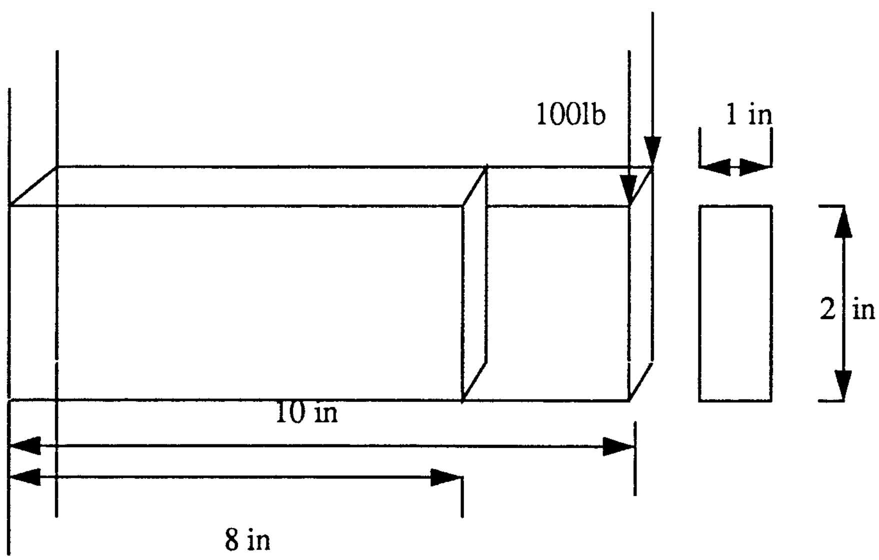

Figure A4.1 Cantilever Beam

A4.2 Calculation Accuracy of I-DEAS

By formular (7.1), the stress on the upper surface at 8 in cross section is

$$\sigma = -\frac{-100 \times 8 \times 1}{\frac{1}{12} 2 \times 1^3} = 48000psi$$

The result calculated by I-DEAS

$$\sigma_{I-DEAS} = 49296psi$$

The error between hand calculation and I-DEAS calculation in this case is 2.7%. Thus, I-DEAS is of enough accuracy.

Appendix 5

The Path of Establishing and Analysising the Mandible Model

All the operations were expressed by I-DEAS screen menu, under the Finite Element Modelling & Analysis Family.

1. Geometry_Model Task (to establish geometry model):

   Geometry_Model: /CREATE-WIRE /POINT /POSITION /K-KEYIN: to key in the coordinate of 64 data points.

   Create_Model: /CREATE-WIRE /LINE OR SPLINE /POINT-TO-PONIT /PICK VISIBLE POINT: to use line or spline to connect the discrete point into a wire geometry shape.

2. Mesh_Generate Task (to establish element mesh)

   Mesh_Volumes: /PICK-UP-AREA: to define the mesh volume for computer to recognize the volume for creation mesh.

   Mesh_Size: /MESH-CREATION /MESH AREAS /DEFAULTS /MESH-TYPE / FREE-MAPPED and /MESH AREAS /SETTING /K-KEY-IN SIZE: by choosing the element type and size, one can decide the calculation result accuracy.

   Mesh_Generate: /MESH-GENERATE: after the above two steps, computer automatically generates elements and nodes.

3. Material-Property Task (to apply elastic constants)

   /MESH-CREATION /MATERIAL PROPERTIES /DIRECTORY /MODIFY /YOUNG MODULUS & POSSION RATIO /K-KEY-IN VALUE: to specify the elastic constants for the problem studied.

4. Boundary_Condition (to apply restraint and structural load)

Restraint: /BOUNDARY-CONDITION /RESTRAINT /GROUP /NEW /ELEMENT /PICK VISIBLE POINT /TRANSPLATE-FREEDOM /ROTATION-FREEDOM /KEY-IN-VALUE: to define the restraint type and specify the restraint location.

Structure_Load: /STRUCTURAL-LOAD /GROUP /NEW /NODE /PICK VISIBLE POINT /KEY-IN-FORCE & MOMENT: to define the force type and specify the force location, both the restraint force and structural load are applied in this menu.

5. Model_Solution (to solve the problem)

Output_Selection: /METHOD /SOLUTION-NO-RESTAR /OUTPUT SELECTION /DISPLCEMENT & STRESS /STORE: to choose the output type (i.e. displacement or stress)

Solve_Linear_Statics: /MODEL-SOLUTION /LINEAR-STATICS /CASE-SET / USE /SOLVE: to specify the type of problem is linear static problem.

Report_Solution_Errors: /REPORT-SOLUTION-ERRORS /COMPLETE-LIST: to report the errors produced in previous steps 1-4.

6. Post_Process (to show out the results)

Group: /GROUP /NEW / ELEMENT /ALL: to specify several or all the elements and nodes for getting output.

Analysis_Dataset_set: /ANALYSIS-DATA-SET /CURRENT /DEFORMED-GEOMETRY & STRESS /CONTOUR /DATA COMPONENT /DISPLACEMENT & MAXIMUM-PRINCIPAL /CONTINUOUS TONE /EXECUTE: to specify the type of data (i.e. displacement or stress) for analysis and choose the contour output.

Manage_Models: /MANAGE-MODEL /STORE /K-KEY-IN /FILE NAME: to save the calculation results or store the output analysis results.

References

1. Farah, J. W., R. G. Craig, and D. L. Sikarski. "Photoelastic and Finite Element Stress Analysis of A Restored Axisymmetric First Molar." *J. Biomechanics* **6** (1973): 511

2. Vijvay, K. G., Satish C. Khere, Heffrey L. Relston, and Kuang H. Chang. "Stresses at the Dentinoenamel Junction of Human Teeth--A Finite Element Investigation." *J. Prosthetic Dentistry* **66** (4) (1991): 451-459

3. Knoell, A. C. "A Mathematical Model of An in *Vitro* Human Mandible." *J. Biomechanics* **10** (1977): 159

4. Gupta, K. K., A. C. Knoell, and D. E. Grenoble. "Mathematical Modeling and Structural Analysis of the Mandible." *Biomaterials, Medical Devices, and Artificial Organs* **1** (1973): 469

5. Weijs, W. A., and B. Hillen. "Cross-sectional Areas and Estimated Intrinsic Strength of the Human Jaw Muscles." *Acta Morph. Neerl.-Scand.* **23** (1985): 267-274

6. Weijs, W. A., and B. Hillen. "Relationship Between the Physiological Cross-section of the Human Jaw Muscles and Their Cross-sectional Area in Computer Tomograms." *Acta Anat.* **118** (1984): 129-138

7. Koolstra, J. H., and T. M. G. J. Vna Eijden. "Application and Validation of A Three Demensional Mathemaical Model of the Human Masticatory System in *Vivo*." *J. Biomechanics* **25** (2) (1992): 175-187

8. Jadranka, Keros-Nagle. "Deformationand Strain Measurements of the Applied Extensor Appliance in the Lower Jaw Model." *Acta Med. Iug* **35** (1981): 285-304

9. Ferre, J. C., R. Legonx, J. L. Helary, *et al.* "Study of the Deformations of the Isolated Mandible under Static Constraints by Simulation on a Physicomathematical Model." *Anat. Clin* **7** (1985): 183-192

10. Umetani, Y., and Morio Inou. "Movement and Function of Mandible -- A Simplified Mechanomorphological Model of Mandible." *Anat. Anz., Jena* **165** (1988): 193-196

11. Throckmortron, Gaylord S., and Linda S. Throckmortron. "Quantitative Calculations of Temporomandibular Joint Reaction Force--I. The Importance of the Magnitude of the Jaw Muscle Forces." *J. Biomechanics* **18**(6) (1985): 445-452

12. Throckmortron, Gaylord S. "Quantitative Calculations of Temporomandibular Joint Reaction Force--II. The Importance of the Direction of the Jaw Muscle Forces." *J. Biomechanics* **18**(6) 1985: 453-461

13. Ashman, R. B., and W. C. Van Buskirk. "The Elastic Properties of A Human Mandible." *Adv. Dent. Res* **1** (1) (1987): 64-67

14. Hart, Richard T., V. Henneben Vincent, Nisra Thongpreda, William C. Van Buskirk, and Ronald C. Anderson. "Modeling the Biomechanics of the Mandible: A Three Dimensional Finite Element Study." *J. Biomechanics* **35** (3) (1992): 261-286

15. Chari and Silvester: *"Finite Elements for Electrical and Magnetics Field Problems."* London: John Wiley, 1980

16. Schwarz, H. R. *"Computational Mathematics and Applications: Finite Element Methods."* London: Academic Press, 1988

17. William, H. Bowes, and Leslie T. Russell. *"Stress Analysis by the Finite Element Methodfor Practicing Engineerings."* Lexington, MA: Lexington Books, 1975

18. Structural Dynamics Research Corporation: *"I-DEAS V Finite Element Modeling and Analysis Menu Guide."*, 1990

19. Agur, Anne M. R. *"Grant's Altas of Anatomy: Chapter 7 the Head." 9th ed.* New York: Williams & Milkins, *1991*

20. Huelke, Donald F. *"Selected Dissections of the Facial Regions for Advanced Dental Students." 6th ed.* Philadelaphia: The Overlook Co., *1991*

21. Anson and McVay. *"Surgical Anatomy."* Vol. 1, *6th ed.* Philadelphia: W. B. Saunders, 1984

22. Shapiro, Harry H. *"Applied Anatomy of the Head and Neck,* Chapter 4: *Musclature of the Face and Jaws."* Philadelaphia: Lippincott. 1973

23. Schultz, Richard Carlton. *"Facial Injuries." 3rd ed.* New York: Year Book Medical Publisher, 1988

24. Warwick, Roger. *"Johnston's Synoposis of Regional Anatomy." 10th ed.* Philadelphia: Lea & Febiger, 1968

25. Osborn, J. W., and F. A. Baragab. "Predicted Pattern of Human Muscle Activity During Clenching Derived from a Computer Assisted Model: Symmetric Vertical Bite Forces." *J. Biomechanics* **18** (8) (1985): 599-612

26. Hylander, William L. "The Human Mandible: Lever of Link." *Am. J. Phys. Anthrop.* **43** (1975): 227-242.

27. Structural Dynamics Research Corporation: *"I-DEAS V Solid Modeling Menu Guide."*, 1990

28. Chuong, Robert C., R. Bruce Donoff, and Walter C. Guaalick. "A Retrospective Analysis of 327 Mandibular Fractures." *Oral Maxillofac Surg* **41** (1983): 305-309

29. Rohl, L., E. Larsen, F. Line, A. Odgaard, and J. Jorgensen. "Tensile and Compressive Properties of Cancellous Bone." *J. Biomechanics* **24** (12) (1991): 1143-1149

30. Odgaard, A., and F. Line. "The Underestimation of Young's Modulus in Compressive Testing of Cancellous Bone Specimens." *J. Biomechanics* **24** (8) (1991): 691-698

31. Bochlogyros, Pantelis Nic. "A Retrospective Study of 1521 Mandibular Fractures." *Oral Maxilofac Surg* **43** (1985): 597-599

32. Baragar F. A., and J. W. Osborn. "A Model Relating Patterns of Human Jaw Movement to Biomechanical Constraints." *J. Biomechanics* **17**(10) (1984): 757-767

33. Bauld, R. Nelson Jr. *"Mechanics of Materials, Chapter 6 Bending of Straight Beams." 2nd ed.* Boston: PWS Engineering, 1986

34. Schmid-Schonbein, G. W., S. L. Y. Woo, and B. W. Zweifach. "*Frontiers in Biomechanics, Chapter 15. Bone Mechanics.*" New York: Spinger-Verlag, 1984